WELL TESTING IN GAS-CONDENSATE RESERVOIRS

A REPORT SUBMITTED TO THE DEPARTMENT OF PETROLEUM ENGINEERING

OF STANFORD UNIVERSITY

IN PARTIAL FULFILLMENT OF THE REQUIREMENTS FOR THE DEGREE OF MASTER OF SCIENCE

By

Rajeev R. Lal

June 2003

I certify that I have read this report and that in my opinion it is fully adequate, in scope and in quality, as partial fulfillment of the degree of Master of Science in Petroleum Engineering.

_____

Prof. Roland N. Horne
(Principal Advisor)

Abstract

Gas-condensate reservoirs differ from dry-gas reservoirs. Understanding of phase and fluid flow behavior relationships is essential if we want to make accurate engineering computations for gas-condensate systems (e.g., well testing, estimating reserves and predicting production trends). Condensate dropout occurs in the reservoir as the pressure falls below dew-point, as a result of which, the production decreases significantly and the condensate bank formed is also unrecoverable. Hence, the condensate saturation and liquid buildup is very significant in gas-condensate reservoirs. However, it has been observed that the saturation buildup across the reservoir is much more than the maximum equilibrium saturation given by the equilibrium phase behavior of the condensate fluid. This study aimed at understanding the multiphase flow behavior in gas-condensate reservoirs and, in particular, investigated the factors that lead to such high saturation buildup in the reservoir. Changes in the fluid composition due to liquid dropout have also been investigated. In particular, we studied the effect of critical condensate saturation and shapes of relative permeability curves on flow and saturation buildup fluid.

Acknowledgments

First and foremost, I would like to thank my advisor, Prof. Roland N. Horne, for his constant support and guidance during this study. I would like to express my sincere gratitude for his patience and encouragement throughout this work, without which this work would not have been possible.

I am extremely grateful to the entire Stanford Petroleum Engineering faculty for their significant contribution to my academic and intellectual development. I firmly believe that they have bettered me as a petroleum engineer and I will carry with me the skills they have given in my future work. Thanks to Dr. Kewen Li for his insightful ideas and suggestions.

Special thanks also go to Saudi Aramco for their monetary and moral support for our research efforts.

I would also like to thank all my friends and colleagues for making my stay at Stanford memorable.

Contents

List of Tables

List of Figures

Chapter 1

1. Introduction

Reservoirs bearing gas-condensates are becoming more common as developments are encountering greater depths, higher pressures, and higher temperatures. Accuracy in engineering computations for gas-condensate systems (e.g., well testing, estimating reserves, sizing surface facilities, and predicting productivity trends) depends upon a basic understanding of phase and flow behavior relationships. When we compare dry- gas reservoirs with gas-condensate reservoirs, there are many special factors that affect the performance of gas-condensate reservoir during the exploitation process.

At the time of discovery, a typical gas-condensate reservoir pressure might be above or close to the critical pressure. At this time there exists only single-phase gas. However as the production is carried out, there is isothermal pressure decline and as the bottom hole pressure in a flowing well falls below the dew-point of the fluid a liquid hydrocarbon phase is formed. This retrograde condensate formation results in buildup of a liquid phase around the wellbore, leading to a decrease in the effective permeability to gas into the wellbore. The productivity loss associated with condensate buildup can be substantial. Afidick et al. (1994) and Barnum et al. (1995) have accounted for several instances in which well productivities have been reported to decline by a factor of two to four as a result of condensate accumulation.

The liquid dropout first occurs near the wellbore and propagates radially away from the well (assuming the well at the center of a radial reservoir) along with the pressure drop. Fevang (1995) and Ali et al. (1997) showed that, when reservoir pressure around a well drops below the dew-point pressure, retrograde condensation occurs and three regions are created with different liquid saturations. Away from the well, an outer region has the initial liquid saturation; next, there is an intermediate region with a rapid increase in liquid saturation and a corresponding decrease in gas relative permeability. Liquid in that

region is less than the critical condensate saturation and hence is immobile. Closer to the well, an inner region forms where the liquid saturation reaches a critical value, and the effluent travels as two-phase flow with constant composition (the condensate deposited as pressure deceases is equal to that flowing towards the well. According to Economides et al. (1987) and Fussel (1973) there may also exist a fourth region in the immediate vicinity of the well where low interfacial tensions (IFT) at high rates yield a decrease of the liquid saturation and an increase of the gas relative permeability.

Understanding the multiphase flow phenomena in such reservoirs is key in characterizing the condensate dropout and subsequent blockage effect. It is generally believed that the flow behavior of gas-condensate in porous media is different from that of gas-oil and water-oil systems. However, the number of reported studies relevant to gas-condensate flow phenomena is limited, and it is quite common to apply information, such as the relative permeabilities and the critical liquid saturation, generated from related studies on gas-oil systems. Gasoline-nitrogen (Eilerts et al., 1967) and water-gas (Naville et al., 1965) systems have been used to simulate gas-condensate flow in cores resulting in estimates of the critical flow saturation ranging from 30% to 50% of the pore volume.

Saeidi and Handy (1974) studied the flow and phase behavior of gas-condensate (methane-propane) in porous media (sandstone core). They indicated that interstitial water shifts the oil's relative permeability to an appreciably lower saturation. In addition, no flow of condensate was observed for this system even with an 18% volumetric condensate dropout in the presence of 30% interstitial water saturation. Asar and Handy (1988) investigated the influence of interfacial tension on the relative permeability of gas/oil in a gas-condensate system. They postulated that the irreducible gas and liquid saturations approach zero as interfacial tension approaches zero. In addition, they observed that condensate could flow at a low condensate saturation (S_{cc} = 10%). Finally, it was concluded that liquid could flow at a very low liquid saturation at low interfacial tensions in a condensate reservoir. This is significant as regions with two-phase (gas and liquid) conditions have low interfacial tension.

Gravier et al. (1983) used the steady-state displacement method with horizontal cores (tight reservoir limestone) with interstitial water saturation from 19.5% to 30%. They

determined the critical condensate saturation (S_{cc}) by injecting gas-condensate into the core. The S_{cc} values ranged from 24.5 to 50%, with interfacial tension ranging from 0.5 to 1.5 mN/m. Danesh et al. (1988) investigated retrograde condensation in water-wet pores in their micromodels and a set of sandstone cores. They determined S_{cc} values of 20.5% to 6.8% in the absence and presence of interstitial water, respectively.

These various studies suggest the minimum required condensate saturation for the flow of condensate is quite high, yet field experiences suggest otherwise. Allen and Roe (1950) reported on the behavior of a gas reservoir with an average water saturation of 30% and a maximum liquid saturation of 12%. They concluded that condensate flowed from the formation into the wellbore throughout most of the reservoir's productive life.

Nikravesh et al. (1996) have accounted for existence of a threshold value or an interval of interfacial tension (0.03-0.05 dyne/cm) in which the shape of the relative permeability curve changes significantly and S_{cc} increases drastically. They also gave account of effect of interstitial water on $S_{cc.}$ Nikravesh et al. (1996) reported that one of the works showed no effect of interstitial water on S_{cc} while another showed negative effect on S_{cc}, and yet another postulated that $S_{cc} + S_{wi}$ is a constant. Unfortunately, even with the limited amount of literature in this area, the conclusions are contradictory and controversial. The contradictions are due to inadequate understanding of chemical and physical processes, especially the adsorption and phase transformation involved in the condensate formation and flow behavior.

O'Dell and Miller (1965) presented a simple method based on steady-state flow concept that can be used to estimate the deliverability from the well. Results obtained using this method indicate that prediction of producing well rates will be pessimistic if the average reservoir pressure is below the saturation pressure of the in-place fluid.

Fussell (1973) described the use of a modified version of one-dimensional radial model developed by Roebuck et al. (1969) to study the long-term single-well performance. The condensate accumulation in the producing region are much greater than those measured experimentally during constant volume depletion (CVD) process.

Hinchman and Barree (1985) studied the effect of the fluid characteristics on the predicted productivity decline of a gas-condensate well. They demonstrated that the amount of gas-condensate accumulation near the wellbore depends greatly on the richness of the gas-condensate, the relative permeability data and the liquid viscosity. Sognesand (1991) discussed the condensate buildup in vertically fractured gas-condensate wells. He showed that the condensate buildup depends on the relative permeability characteristics and production mode, increased permeability to gas yields reduced amount of condensate accumulation, and constant pressure production yields the largest near fracture condensate buildup.

Jones, Vo, and Raghavan (1989) studied theory of the steady-state flow for gas-condensate reservoirs. The relationship between the oil saturation and pressure they presented is the same as that Chopra et al. (1986) had given. A no-flow region for condensate liquid was not allowed (only two zones were considered, one where there is only single-phase reservoir fluid and it is mobile and the other near the wellbore that has both gas and condensate present and both phases are mobile) and the condensate saturation values Jones et al. (1989) gave are much greater than the critical saturation.

In the retrograde condensate region, the interfacial tension between the gas and the condensed phase is very small. Hence, it is expected that the capillary forces, which are the major factor governing multiphase flow behavior in reservoirs, play a less important role relative to both gravity and viscous (shear) forces.

These studies show the significance of condensate saturation and the liquid buildup across the reservoir. Productivity above the dew-point pressure is controlled by the reservoir permeability and thickness, and by the viscosity of the gas. Below the dew-point, the degree of productivity will be controlled by the critical condensate saturation (S_{cc}) and the shape of the gas and condensate relative permeability curves. It has also been observed that the saturation buildup across the reservoir is much more than the maximum equilibrium saturation given by phase behavior of the condensate fluid. The liquid saturation is also different from the critical condensate saturation. This study aims at understanding the multiphase flow behavior in gas-condensate reservoirs and, in particular, the effects of critical condensate saturation, shapes of relative permeability

curves and the effect of capillary forces have been investigated. The effect of different S_{cc} values on the saturation profile across the reservoir and the changing fluid composition is presented. The sensitivity of relative permeability curves on saturation build up and the fluid compositional changes is also presented.

Chapter 2 discusses the multiphase flow phenomena in gas-condensate reservoirs. The phase and drawdown behavior of gas-condensate fluids is also presented. In Chapter 3, the various parameters and procedures used, to study and investigate the saturation buildup and compositional changes, are presented. Results and discussions of the effect of the different parameters on saturation profile are presented in Chapter 4. Chapter 5 shows the conclusions made during this study.

Chapter 2

2. Flow Behavior in Gas-Condensates

2.1. Gas-Condensate Fluid Properties

A reservoir fluid is classified as:

- Dry gas when the reservoir temperature is greater than the cricondentherm and surface/transport conditions are outside the two-phase envelope.

- Wet gas when the reservoir temperature is less than the cricondentherm and greater than the critical temperature.

- Oil (volatile or black oil) when the reservoir temperature is less than the mixture critical temperature.

Table 2.1 compares the molar compositions and properties of gas-condensates with other reservoir fluids. For a given reservoir temperature and pressure, Figure 2.1 shows the spectrum of reservoir fluids from wet gas to black oil expressed in terms of gas-oil ratio (GOR) and oil-gas ratio (OGR). A more quantitative classification is also given in Figure 2.1 in terms of molar compositions, by use of a ternary diagram. Retrograde gas-condensate reservoirs typically exhibit gas-oil ratios between 3,000 and 150,000 scf/STB (oil-gas ratios from about 350 to 5 STB/MMscf) and liquid gravities between 40 and 60° API.

Table 2.1: Composition and properties of several reservoir fluids (Monograph vol. 20, SPE).

Composition (mol%)						
Component	Dry Gas	Wet Gas	Gas Condensate	Near-Critical Oil	Volatile oil	Black oil
CO_2	0.10	1.41	2.37	1.30	0.93	0.02
N_2	2.07	0.25	0.31	0.56	0.21	0.34
C_1	86.12	92.46	73.19	69.44	58.77	36.42
C_2	5.91	3.18	7.8	7.88	7.57	4.11
C_3	3.58	1.01	3.55	4.26	4.09	1.01
i-C_4	1.72	0.28	0.71	0.89	0.91	0.76
n-C_4		0.24	1.45	2.14	2.09	0.49
i-C_5	0.50	0.13	0.64	0.90	0.77	0.43
n-C_5		0.08	0.68	1.13	1.15	0.21
$C_{6(s)}$		0.14	1.09	1.46	1.75	1.61
C_{7+}		0.82	8.21	10.04	21.76	56.40
Properties						
$M_{C_{7+}}$		130	184	219	228	274
$\gamma_{C_{7+}}$		0.763	0.816	0.839	0.858	0.920
K_{WC_7}		12.00	11.95	11.98	11.83	11.47
GOR, scf/STB	∞	105,000	5,450	3,650	1,490	300
OGR, STB/MMscf	0	10	180	275		
γ_{API}		57	49	45	38	24
γ_g		0.61	0.70	0.71	0.70	0.63
p_{sat}, psia		3,430	6,560	7,015	5,420	2,810
B_{sat}, ft^3/scf or bbl/STB		0.0051	0.0039	2.78	1.73	1.16
ρ_{sat}, lbm/ft^3		9.61	26.7	30.7	38.2	51.4

2.2. Flow Behavior

2.2.1. Phase Equilibrium

The term "retrograde condensation" is used to describe the anomalous behavior of a mixture that form a liquid by isothermal decrease in pressure or by an isobaric increase in temperature.

Figure 2.2 is a constant-composition p-T projection of a three-component system. The diagram shows lines of constant liquid volume percent (quality). Although total composition is fixed, the respective compositions of saturated vapor and liquid phases change along the quality lines. The bubble-point curve represents the locus of 100% liquid, and the dew-point

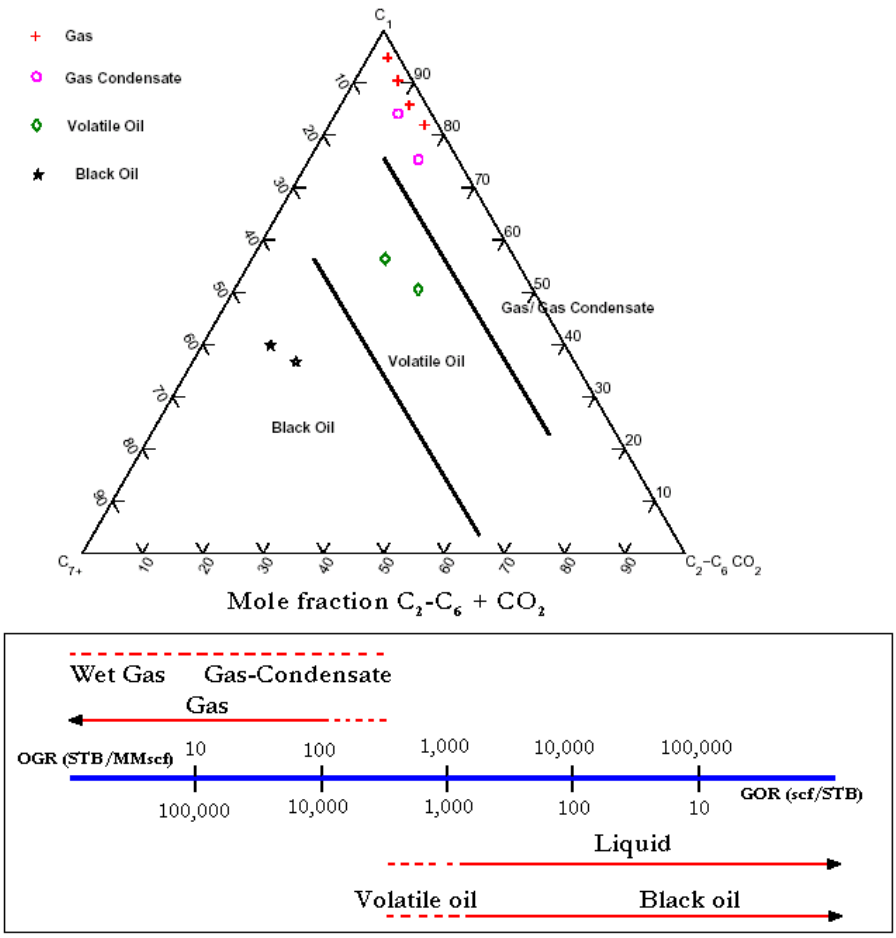

Figure 2.1: Ternary diagram of hydrocarbon fluid and speactrum of reservoir fluids from wet gas to black oil expressed in terms of GORs and OGRs (Monograph vol. 20, SPE)

curve represents the locus of 0% liquid. The regions of retrograde behavior are defined by the lines of constant quality that exhibit a maximum with respect to temperature or pressure. Figure 2.2 shows that for retrograde phenomena to occur, the temperature must be between the critical temperature and the cricondentherm. If the initial reservoir condition were represented by point A1 on the pressure-temperature phase diagram of Figure 2.2, then the isothermal pressure decline during reservoir depletion would follow the line A1-A4. Because the initial reservoir pressure is above the upper dew-point pressure, the hydrocarbon system exists as a single phase (i.e., vapor phase) and remains so during the isothermal decline path A1-A2. As the reservoir pressure drops below point A2, the dew-point will be passed and a liquid phase will develop in the reservoir. Liquid

dropout will continue to increase and reaches a maximum dropout at point A3. However, at point A4, the dew-point curve must be crossed again. This means that all the liquid, which formed, must vaporize because the system is essentially all vapor at the lower dew-point.

These comments assume that the overall composition of the reservoir mixture remains constant during depletion, a reasonable assumption in the context of this general discussion. In reality, however, the behavior of liquid dropout and revaporization differs from that suggested by constant-composition analysis. The retrograde liquid saturation is usually less than the saturation needed to mobilize the liquid phase. Because the heavier components in the original mixture constitute most of the (immobile) condensate saturation, the overall molecular weight of the remaining reservoir fluid increases during depletion. The phase envelope of this heavier reservoir mixture is pushed down and to the right of the original phase diagram, the critical point is shifted to the right toward a higher temperature.

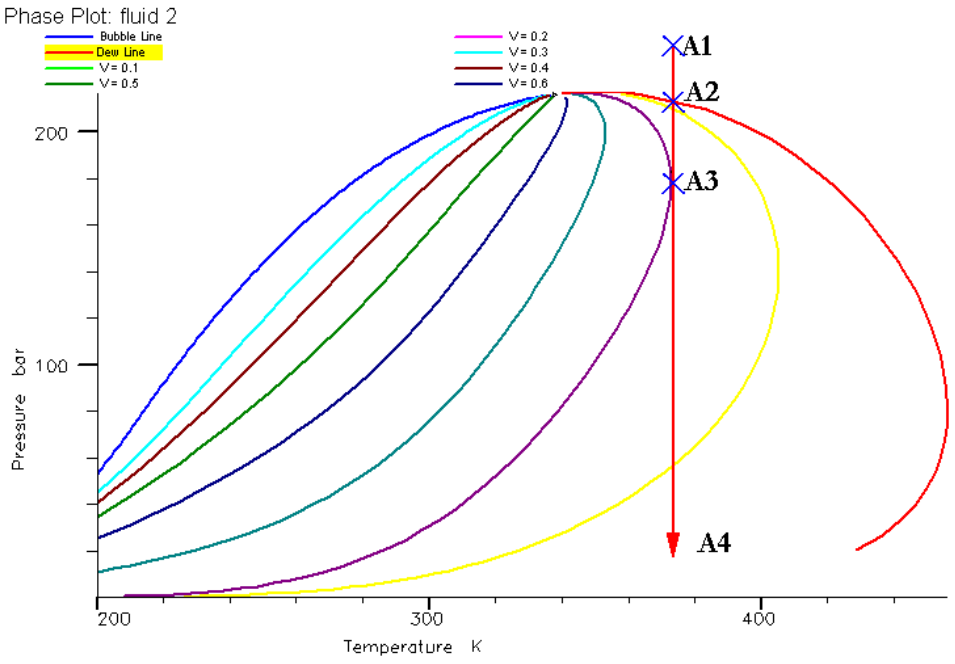

Figure 2.2: Phase envelope diagram of gas-condensate mixture (fluid 2).

Figure 2.3 shows the shift in phase envelope of the well-block gas-condensate mixture with time. The leftmost curve is the original reservoir fluid. The curves on the right of it in the diagram, are after time periods of 1, 10, and 102 days. The points on these curves are the respective critical points. It was observed that the most significant shift in phase envelope occured as soon as within one day. It is not unusual that a retrograde-condensate composition would exhibit a bubble-point pressure if the reservoir were repressured (i.e., the overall mixture critical temperature becomes greater than the reservoir temperature). This change in overall reservoir composition results in less vaporization at lower pressures.

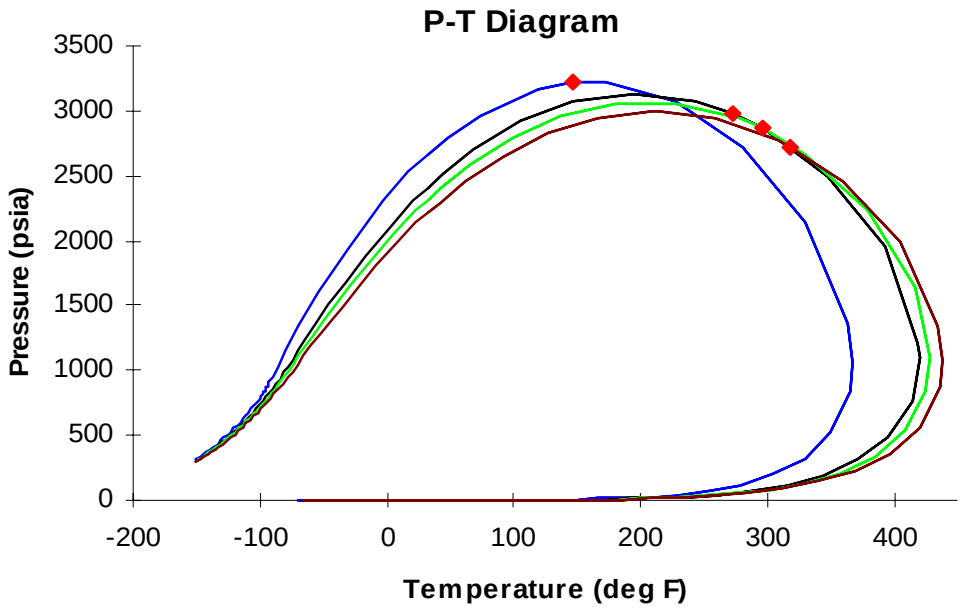

Figure 2.3: Shift in phase envelope of gas-condensate mixture (fluid 2) in the well-bock as the heavier components are dropped out in reservoir.

2.2.2. Retrograde Condensation in Porous Media

Several authors have studied the effect of porous media on the phase behavior of reservoir fluids. Sigmund et al. (1973) investigated the effect of porous media on phase behavior of C_1/n-C_4 and C_1/n-C_5. Their measurements on dew-point, bubble-point pressures, and

equilibrium compositions showed no effect of porous media in moderate surface curvature and pore size larger than several microns.

In conclusion, the equilibrium composition and saturation pressure of retrograde gas-condensate in porous media do not change significantly from their flat surface values except at very high interfacial tension and when the radius of the pore becomes of the order of 0.1 microns and less (i.e., very high surface curvature). Such curvature and very high interfacial tensions are unlikely in hydrocarbon reservoirs.

2.2.3. Drawdown Behavior

As the average pressure in a gas-condensate reservoir continues to decline on production, condensate dropout occurs across the reservoir. An accurate yet simple model of a gas-condensate well undergoing depletion consists of three flow regions (Fevang and Whitson, 1995).

- *Region 1*: An inner near-wellbore region where both gas and liquid flow simultaneously (at different velocities).

- *Region 2*: A region of condensate buildup where only gas is flowing.

- *Region 3*: A region containing single-phase (original) reservoir gas. This region is the farthest away from the well.

For a given producing condition, one, two, or all three regions may exist. These three regions define pseudosteady-state flow conditions, meaning that they represent steady-state conditions at a given time but that the steady-state conditions change gradually during depletion. Figure 2.4 shows the schematic representation of gas-condensate flow during production. The three regions are identified with a block representation of condensate accumulation and mobile phases in the three regions.

Region 1: The condensate saturation in this region is above the critical condensate saturation (S_{cc}) and hence both gas and liquid phases are mobile. The flowing composition (GOR) within Region 1 is constant throughout. That means that the single-

phase gas entering Region 1 has the same composition as the produced wellstream mixture. Conversely, if we know the producing wellstream, then we know the flowing composition within Region 1. Furthermore, the dew-point of the producing wellstream mixture equals the reservoir pressure at the outer edge of Region 1.

Region 1 is the main source of deliverability loss in a gas-condensate well. Gas relative permeability is reduced drastically in this region due to condensate buildup. The reduction in relative permeability to gas is the most in this region. Even though condensate buildup starts from Region 2, the liquid phase is immobile. Two-phase flow in Region 1 is the main cause of gas relative permeability reduction. The size of Region 1 increases with time. For steady-state conditions, the condensate saturation in Region 1 is determined (as a function if radius) specifically to ensure that all liquid that condenses from the single-phase gas entering Region 1 has sufficient mobility to flow through and out of Region 1 without any net accumulation. Since the composition of the flowing mixture is constant throughout Region 1, the liquid saturation could be calculated by a constant composition expansion of the producing fluid. The amount of liquid dropout in Region 1 depends primarily on the PVT properties of the gas-condensate mixture and the production rate.

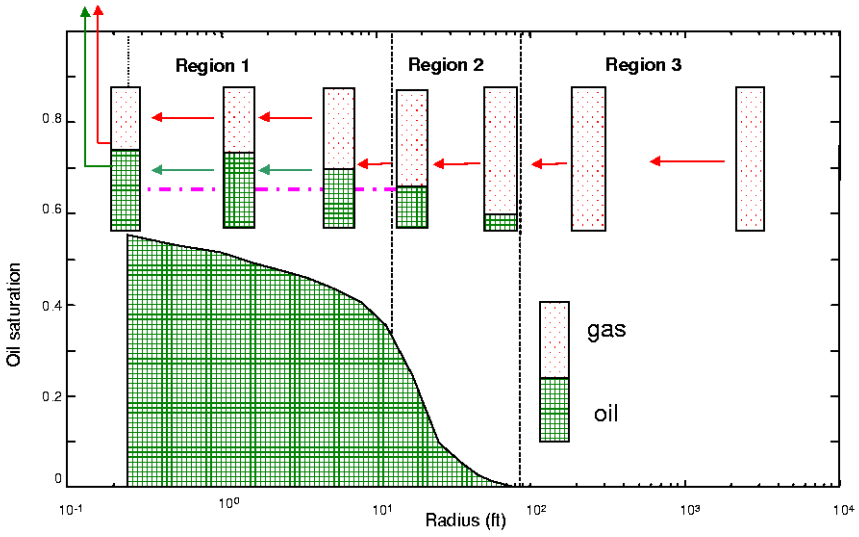

Figure 2.4: Schematic gas-condensate flow behavior (Roussennac, 2001).

Region 2: This is the intermediate zone where condensate dropout begins and it defines a region of net accumulation of condensate. The condensate saturation is below the critical value (S_{cc}) and, effectively, only gas is flowing in this region because oil mobility is zero (or very small). Condensate saturations in Region 2 are closely approximated by the liquid dropout curve from a constant volume depletion (CVD) experiment, corrected for water saturation.

The size of Region 2 is largest at early times just after the reservoir pressure drops below the dew-point. Region 2 decreases with time because Region 1 is expanding. The size and importance of region 2 is greater for lean gas-condensate. The critical condensate saturation (S_{cc}) also affects the size of Region 2. The size of this region increases for increasing values of S_{cc}. Hence, S_{cc} is significant in studying the changing composition of the fluid because Region 2 has a constantly changing composition of the reservoir fluid. The main consequence of Region 2 is that producing wellstream composition (GOR) is leaner than calculated by a simple volumetric material balance (e.g., CVD measurements).

Region 3: This is the region farthest away from the well where reservoir pressure exceeds the dew-point pressure of the original reservoir fluid. Single-phase gas is present and hence is the only mobile phase.

Coexistence of Flow Regions: Initially, when the reservoir pressure is above the dew-point, the whole reservoir is Region 3. As the reservoir is depleted, Regions 2 and 1 appear depending on the condensate buildup across the reservoir. If bottom hole flowing pressure (BHFP) is less than the dew-point, Region 1 will always exist (after a short transient required to buildup the steady-state saturations in Region 1). Region 1 will not exist if flowing bottom hole pressure is greater than the dew-point.

Region 2 will always exist together with Region 1 after reservoir pressure drops below the dew-point. In this case Region 3 will not exist. All three regions exist for reservoirs that are slightly undersaturated and BHFP is less than the dew-point. Region 2 may "disappear" or have negligible effect for highly undersaturated reservoirs. Region 2 is negligible or very small for rich gas-condensates.

It is not possible for Regions 2 and 3 to exist in the absence of Region 1 (after steady-state conditions are reached). For a very rich (near-critical) gas-condensate, region 1 may exist throughout the drainage area (in the absence of Regions 2 and 3), after reservoir pressure drops below the dew-point.

2.2.4. Three Region Flow as Function of Time

In the previous section, we discussed the different flow regions across the reservoir. However, these flow regimes may also be observed at any specific point in a reservoir as a function of time. Figure 2.5 shows the well-block oil saturation and pressure history and how the three flow regions appear with pressure decline. Initially, when the reservoir pressure is above dew-point, there is only single-phase gas flow.

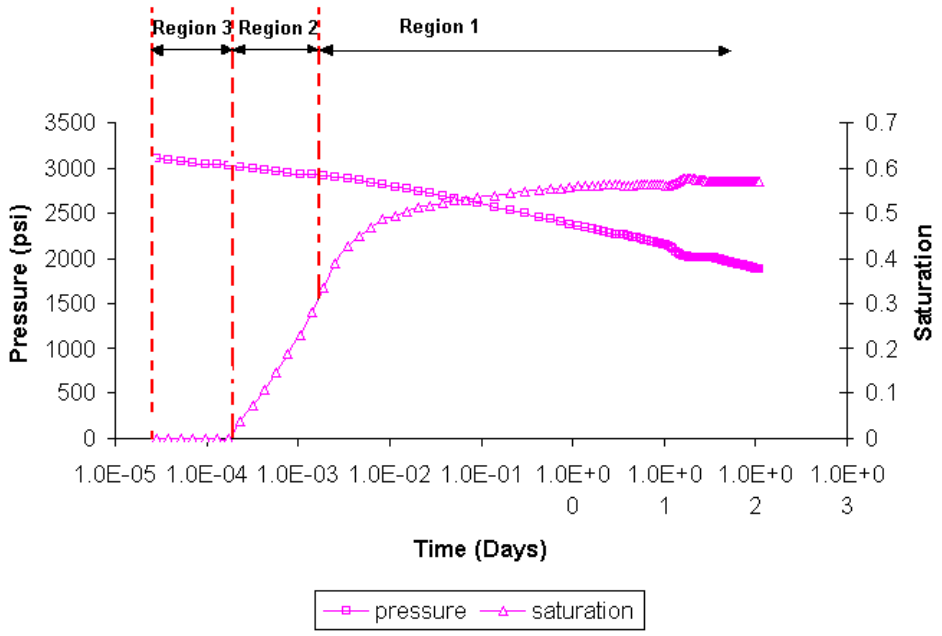

Figure 2.5: Well-block oil saturation and pressure with time.

However, due to high pressure drop near the wellbore, the reservoir pressure would drop below the dew-point and condensate dropout would take place. Region 2 is represented by the time between the first liquid dropout and the time it takes to reach the critical condensate saturation (S_{cc}), after which there will be Region 1 only. Regions 2 and 3 will be quite short (in terms of time) near the wellbore. However, they will increase in time as we move away from the wellbore. This is because there is more drastic pressure drop near the wellbore as compared to the rest of the reservoir. Hence, we would expect the Region 1 to develop quickly near wellbore while there is still Region 3 in other parts of the reservoir.

Chapter 3

3. Parameters and Procedure

3.1. Condensate Banking

Understanding of the multiphase flow phenomena is key to characterization and development of gas-condensate reservoirs. As the pressure of the wellbore falls below the dew-point of the condensate fluid, liquid dropout occurs due to retrograde condensation. This results in liquid saturation buildup, starting from the wellbore and moving away from it with time. Depending on the value of critical condensate saturation (S_{cc}), the liquid phase maybe mobile or immobile. Even if the liquid is immobile (Region 2), this may reduce the relative permeability to gas. However, the magnitude of this is not fully understood. As liquid dropout continues, the producing wellstream gets leaner as more and more heavier components are deposited in the reservoir.

When the liquid saturation exceeds the critical condensate saturation, both gas and liquid phases are mobile (Region 3). Moving liquid phase reduces the relative permeability to gas drastically and hence the well deliverability also decreases. Once the liquid is mobile, the producing composition (GOR) reaches a constant value (higher GOR than the original fluid). This phenomenon of condensate dropout is referred to as “condensate banking”. Condensate banking decreases the gas production and also the dropped out liquid in the reservoir becomes unrecoverable. Which means that the dropped out liquid cannot be revaporized and produced, even if the reservoir pressure is increased by gas injection to a value above the dew-point.

It has been observed that the liquid saturation builds up to a value much higher than that given by maximum phase equilibrium dropout. Figure 3.1 shows the saturation and

pressure profile and GOR across the reservoir for fluid 2 and its corresponding phase envelope. This value is also much more than the critical condensate saturation (S_{cc}). We want to investigate this issue of saturation buildup and study the parameters that may lead to its reaching a *particular value* for a given reservoir fluid and production mode. In this study, we investigated the effect of S_{cc}, relative permeability curves and capillary pressure on the saturation profile.

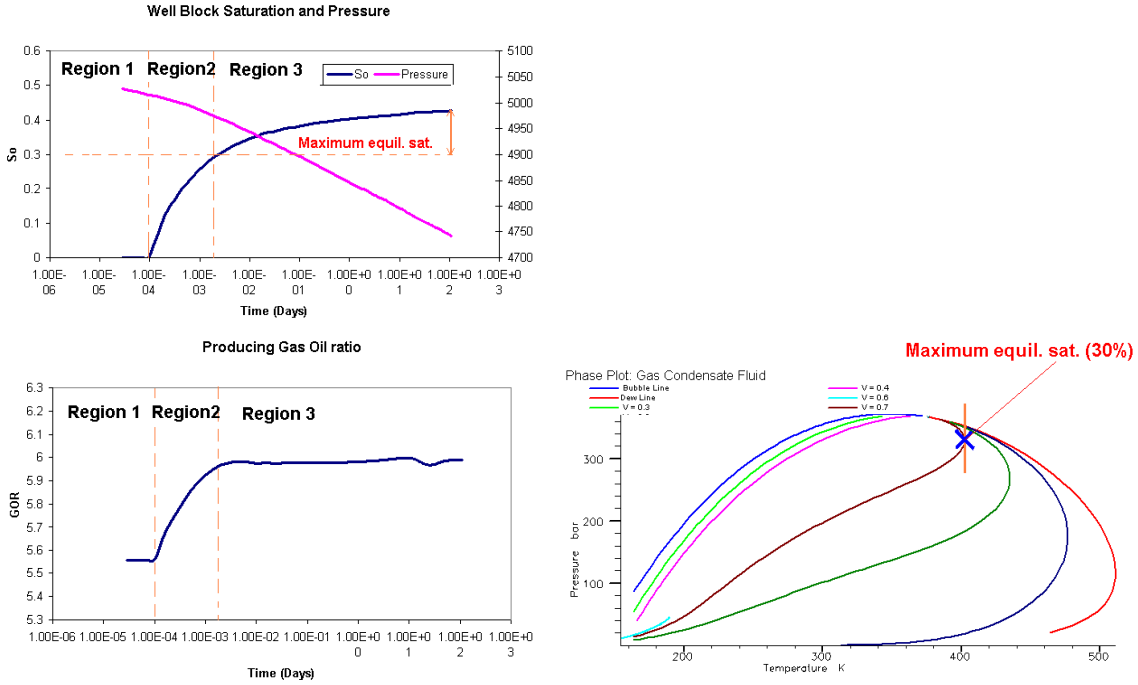

Figure 3.1: Saturation and pressure profile and GOR across the reservoir and the corresponding phase envelope for fluid 2.

3.2. Compositional Changes

As the heavier components are dropped out in the reservoir, the composition of the producing wellstream changes. If we talk of a particular grid block, the composition changes once the grid block pressure is below the dew-point pressure (p_{dew}). The overall composition in the Region 1 and 2 will be richer than the original reservoir fluid. We will be studying the compositional changes in the liquid and vapor phases along with the changes in the overall composition.

3.3. Relative Permeability Curves

It has already been discussed in the literature that relative permeability curves affect the flow significantly in a gas-condensate reservoir once the pressure falls below dew-point pressure (p_{dew}). Accurate knowledge about relative permeability curves in a gas-condensate reservoir would be ideal information. Usually, this is not the case, as the relative permeability curves are rarely known accurately. It would be worthwhile if we could investigate the effect of different relative permeability curves and study the uncertainty they bring to the saturation buildup in gas-condensate reservoirs.

3.3.1. Types of curves used

Different sets of relative permeability curves were used in the study. One of them is the Brooks-Corey relative permeability curves:

$$k_{ro} = k_r(S_{wi})(S_o^*)^2(\frac{S_o}{1-S_{wi}})^{(2+\lambda)/\lambda}$$

(2.1)

$$k_{rg} = k_r(S_{wi})(S_g^*)^2[1-(1-S_g^*)^{(2+\lambda)/\lambda}]$$

(2.2)

where

$$S_o^* = \frac{S_o - S_{oc}}{1-S_{wi}-S_{oc}} \qquad \text{and} \qquad S_g^* = \frac{S_g}{1-S_{wi}}$$

(2.3)

Different sets of relative permeability curves were generated using the Corey equations for different values of S_{cc}. To investigate the effect of critical condensate saturation, X-curves

were used. Figure 3.2 shows the Corey type curves and the X-curve for S_{cc} = 0. X-curves do not include any interaction between gas and liquid phases and the interfacial tension in this case will be zero. Hence, use of such a curve would give the saturation profile had the two phases not been interacting with each other. Figure 3.3 shows X-curves and Corey relative permeability curves for S_{cc} = 0.3 and 0.5.

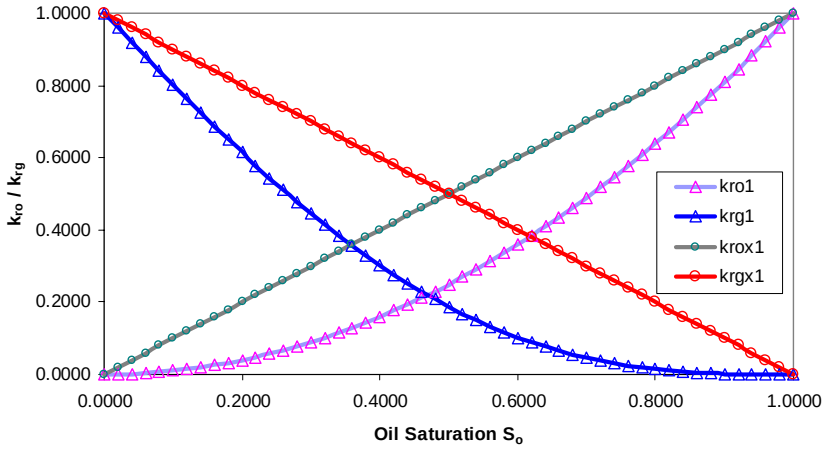

Figure 3.2: Corey and X relative permeability curves for S_{cc} = 0.

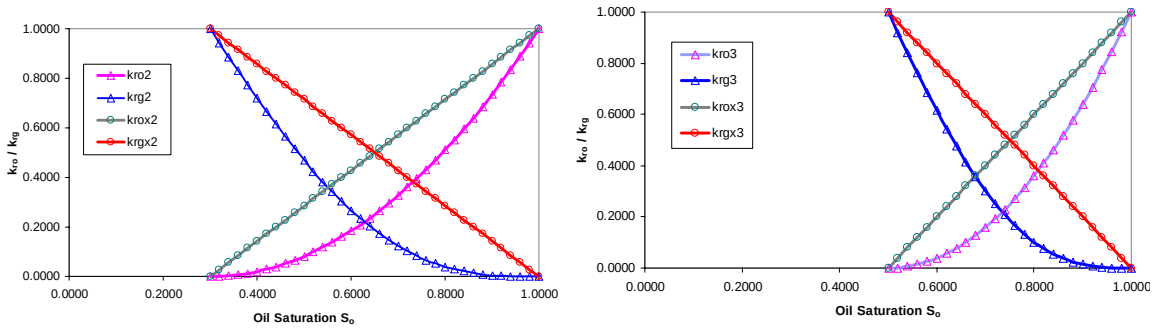

Figure 3.3: Corey and X curves for S_{cc} = 0.3 and 0.5.

Curves with reduced end-point permeability were also generated. **Figure 3.4** shows one such curve for S_{cc} = 0.30.

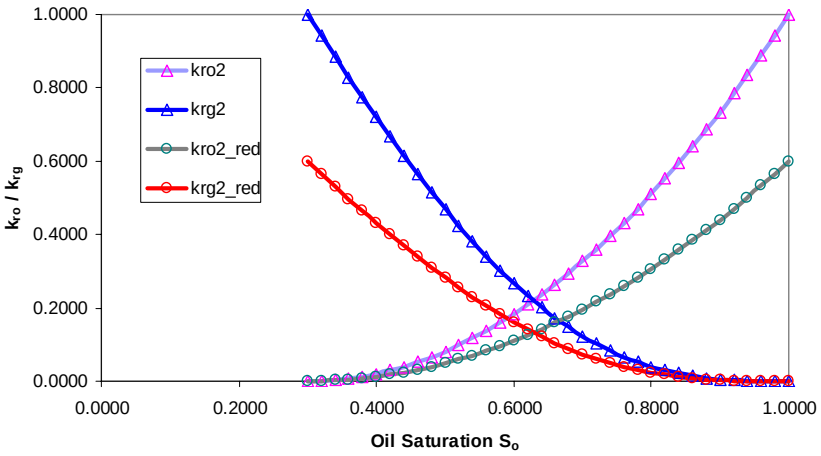

Figure 3.4: Corey curves with reduced end-point relative permeability.

To see how the value of critical condensate saturation affects the saturation profile, the two types of curves with same S_{cc} value were used.

3.3.2. Introduction of capillary pressure in relative permeability curves

The effect of capillary pressure has also been investigated in this study. Li and Horne (2003) have shown that the uncertainty in relative permeability can be reduced if the number of input parameters is decreased. This may be realized by imposing only capillary pressure data as input to numerical simulators. Here, only capillary pressure data need to be specified and the relative permeabilities can be calculated consistently using specific models. Li and Horne (2003) found that the Purcell model (1949) was found to best fit the experimental data of the wetting phase relative permeability. In this study we followed their method and calculated the wetting phase (condensate) relative permeability using the Purcell model and the nonwetting phase (gas) relative permeability using the Brooks-Corey model.

The wetting phase relative permeability was calculated using the following equations:

$$k_{rw} = (S_w^*)^{(2+\lambda)/\lambda} \quad \textbf{(2.4)}$$

where k_{rw} and S_w^* are the relative permeability and the normalized saturation of the wetting phase; λ is the pore size distribution index.

Capillary pressure is calculated using the following equation:

$$P_c = p_e (S_w^*)^{-1/\lambda}$$

(2.5)

Where p_e is the entry capillary pressure. The normalized saturation of the wetting phase in drainage cases is given by:

$$S_w^* = \frac{S_w - S_{wr}}{1 - S_{wr}}$$

(2.6)

Where S_w and S_{wr} are the specific saturation and the residual saturation for wetting phase. For nonwetting phase, relative permeability was calculated using the Brooks-Corey model and can be given by

$$k_{rnw} = (1 - S_w^*)^2 [1 - (S_w^*)^{\frac{2+\lambda}{\lambda}}]$$

(2.7)

Capillary pressure curves shown in Figure 3.5 have been obtained using Eq. 2.5 with same value of p_e but with different values of λ ranging from 2 to 7.

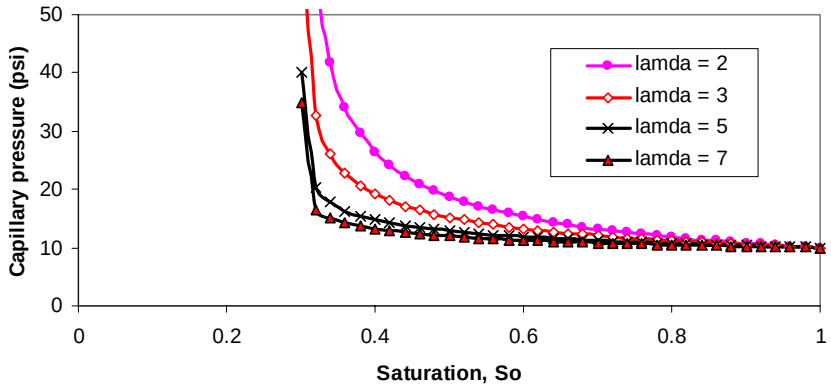

Figure 3.5: Gas oil capillary pressure curves for different of pore size distribution index λ.

3.4. Reservoir Description

The Eclipse 300 compositional simulator was used for simulation. The three-parameter Peng-Robinson equation of state was used to simulate the PVT properties of the gas-condensate fluid. Simulation was carried out for two cases, one with constant rate of production and the other with constant bottom hole flowing pressure as the mode of production. The results are presented for both of these cases.

A one-dimensional radial reservoir model with a single vertical layer and uniform porosity and permeability was used as a test case. A single producer well lies at the center of the reservoir and is assumed to be perforated across the height of the reservoir. The pressure transient information occurs during the first hours of the test, and the near wellbore region is of great interest. Roussennac (2001) has reported that the change of size between two adjacent cells can create numerical instability even with an implicit formulation. The choice of the grid size distribution has to be such that these instabilities are minimized. The numerical simulation should therefore be performed on very small grid blocks around the well using very small time steps. However, since the reservoir volume to be simulated is very large, a distribution of grid cell size has to be chosen (usually radial grid using logarithmic size distribution).

The reservoir is considered to be infinite during the simulation, as the well never feels the reservoir boundary. The properties of the reservoir are given in Table 3.1.

Table 3.1: Reservoir properties used in simulation.

Porosity (%)	20
Absolute permeability (md)	5
Reservoir height (ft.)	30
Irreducible water saturation (%)	0
Reservoir Area (acres)	1950
Rock Compressibility (psi^{-1})	4.10^{-6}

3.5. Fluid Description

A three-component synthetic gas-condensate fluid was used in the simulation. The three components are methane (C_1), n-butane (C_4), and n-decane (C_{10}). Different compositions of these components were used to obtain lean and rich condensate mixtures.

The phase behavior was simulated using three parameter Peng-Robinson equation of state with volume correction. The various compositions we considered enabled us to incorporate all-important features (relevant to phase behavior) of the problem (saturation profile, well productivity, well test analysis). Table 3.2 gives the composition and properties of the condensate fluids. We used Peng-Robinson equation of state to simulate laboratory experiments such as constant composition expansion (CCE) and constant volume depletion (CVD).

Table 3.2: Composition and properties of the condensate fluids used.

Condensate Mixture	fluid 1	fluid 2	fluid 3	fluid 4	fluid 5
C_1	75%	75%	75%	75%	87%
n-C_4	24%	20%	15%	10%	1.50%
n-C_{10}	1%	5%	10%	15%	11.50%
T_c (^oF)	96	148.4	252	247.7	200.3
p_{dew} (psi)	2255	3133	3742	3779	5317

3.6. Constant Rate vs. Bottom Hole Pressure

Two modes of production were carried out and the particular values are discussed here. The well was produced at constant molar rate. The rate was varied to investigate the effect of increased flow rate on saturation profile. It has been documented by some authors that increased flow rate may cause “velocity stripping” resulting in improved production rates.

One of the advantages of constant rate over constant bottom hole flowing pressure is that we can actually see how the fluid saturation and compositions change as the well-block pressure falls below dew-point pressure (p_{dew}). In the constant bottom hole flowing pressure case, in order to have two-phase flow, the bottom hole flowing pressure has to be set below the dew-point pressure, as a result of which, the well-block will have instantaneous liquid buildup as the production is started. However, with constant bottom hole flowing pressure, we can actually see how the fluid flow occurs for different pressures below the dew-point pressure on the phase envelope. Also, we can study the effect of different parameters (e.g. capillary pressure) on well productivity index in this case.

3.7. Laboratory versus Field Scale Simulation

For study of flow phenomena in gas-condensate reservoirs, a radial reservoir model with a single well at the center was used for simulation purposes (Figure 3.6). This is the case as in an actual field and simulates the radial flow of the reservoir fluid towards the well at the center. In the field case, the radial flow option in Eclipse 300 was used, which simulates the flow in radial direction. Single layer radial grid blocks were used in this case. However, the experiments in the laboratory are carried out at core scale. Hence, it will be of particular interest to see how the actual field scale simulations relate to the laboratory scale core simulations.

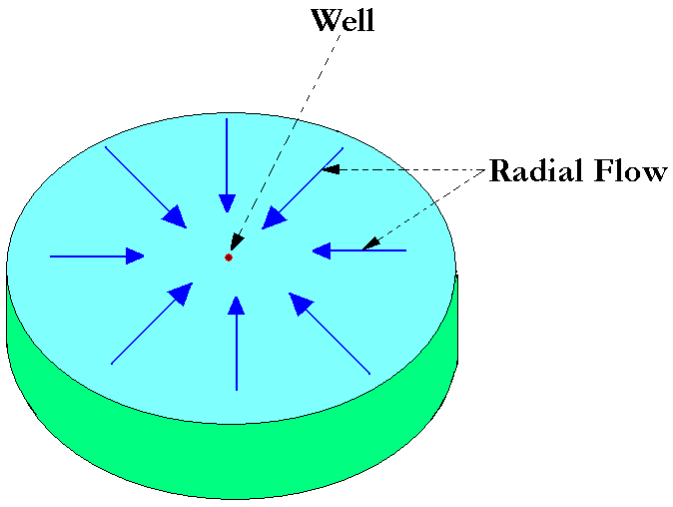

Figure 3.6: Gas–condensate reservoir with single well at center.

In all the experiments regarding gas-condensates, cylindrical core plugs will be used in the laboratory. Figure 3.7 shows one such core plug. The input to the core will be the original single- phase reservoir fluid, however, the output will be two phase *viz* liquid and gas. Hence, the flow is linear for the cylindrical core plug.

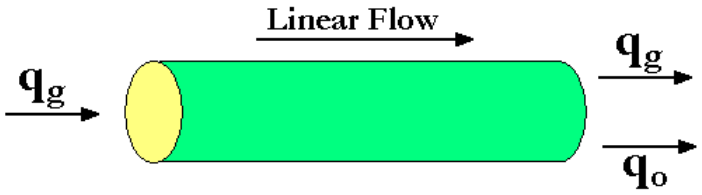

Figure 3.7: Cylindrical core plug used for experiments.

For simulation in the linear direction, we need the grid blocks in Cartesian coordinates. Thus for simulation, the core was approximated with a cubical bar as shown in Figure 3.8, with grid blocks in X, Y and Z directions. The flow is only in the X-direction. The core was divided into 30 grid blocks in the X-direction and one each in the Y- and Z-directions. Smaller grid blocks were considered near the well and then grid sizes increased away from the well. Also, the initial time steps were very small and increased for later time steps.

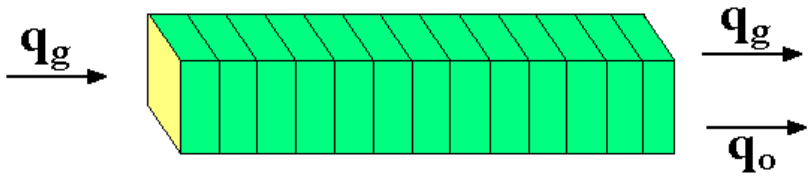

Figure 3.8: Core plug approximated by cubical bar for simulation.

One significant difference between the two cases is the nature of the flow. We considered radial flow in the field scale simulation and linear flow in the laboratory scale. In the next chapter, the results will be discussed as to how the flow mechanism governs the saturation buildup and the resulting compositional changes.

Chapter 4

4. Results and Discussion

The saturation profile and the resulting compositional changes were studied by varying different parameters. Two modes of well control were investigated, constant rate production and production at constant bottom hole flowing pressure (BHFP).

4.1. Constant Rate

The well was produced at constant total molar rate of 6000 lb-mole/day. This rate was chosen after careful simulation runs, by studying the resulting pressure drop on the phase envelope plot of the condensate mixture and ensuring that the final bottom hole flowing pressure lies in the retrograde region.

4.1.1. Relative Permeability Curves

The effect of relative permeability curves was studied by keeping S_{cc} the same and varying the relative permeability curves. Figure 4.1 shows the saturation profile across the reservoir for Brooks-Corey and the X-curves for S_{cc} = 0.3. It was observed that the saturation profile was same irrespective of the relative permeability curve until the value of S_{cc}. At this point, the two profiles deviate and then reach different final saturation values. Figure 4.2 shows the compositional changes across the reservoir in this case. Both C_4 and C_{10} are the heavier fractions and their compositions changes are identical. Hence, only methane (C_1) and n-propane (C_4) compositions have been shown.

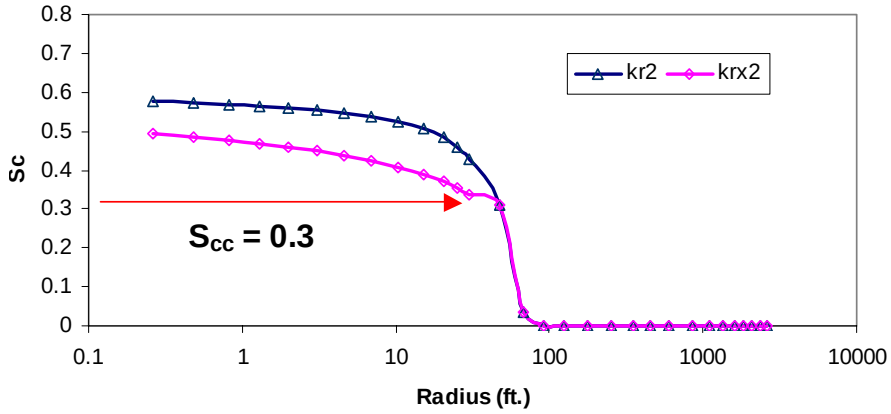

Figure 4.1: Saturation profile across reservoir for Corey (Δ) and X-curves (◊) at S_{cc} = 0.3.

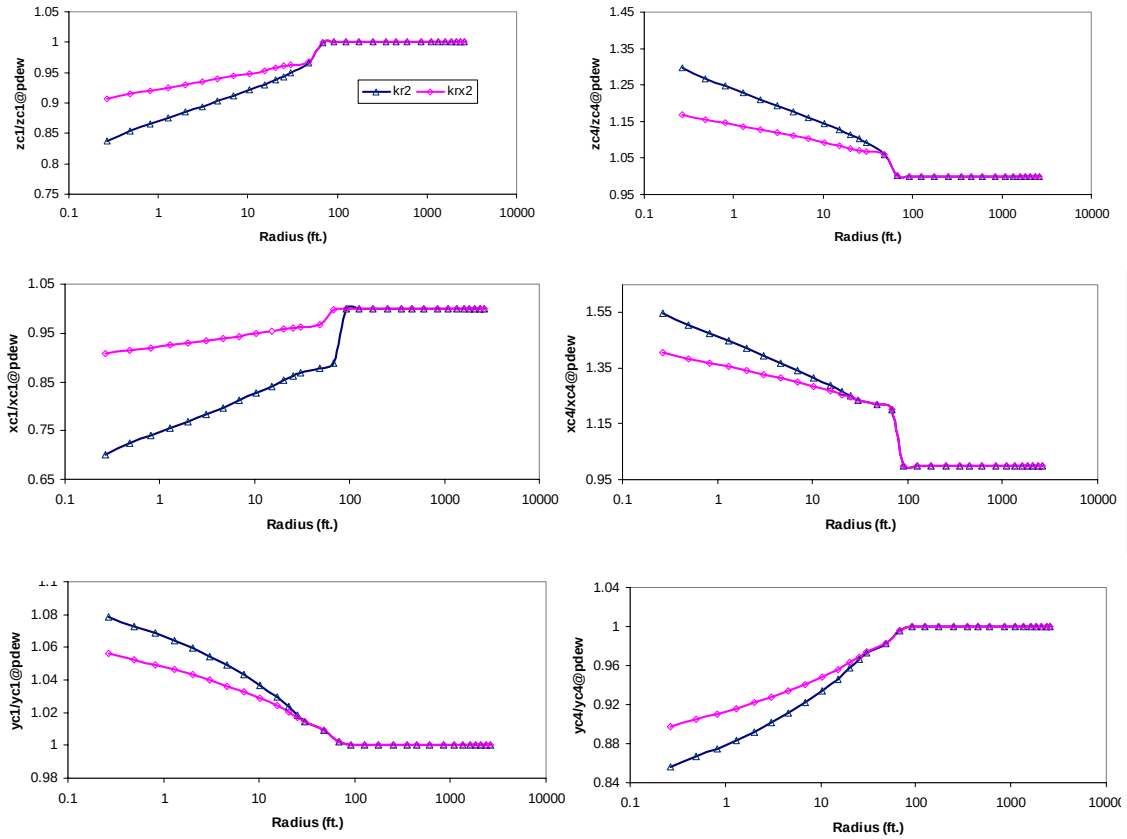

Figure 4.2: C_1 and C_4 compositional change across reservoir for Corey (Δ) and X-curves (◊) at S_{cc} = 0.3.

This phenomenon was also observed for S_{cc} = 0.5 (Figure 4.3), in which case the two profiles follow same path until the liquid saturation is 50% after which they deviate. The resulting changes in the C_1 mole fraction are shown in Figure 4.4. It is observed that the changes in composition of the components are more for higher S_{cc} values (bigger Region 2).

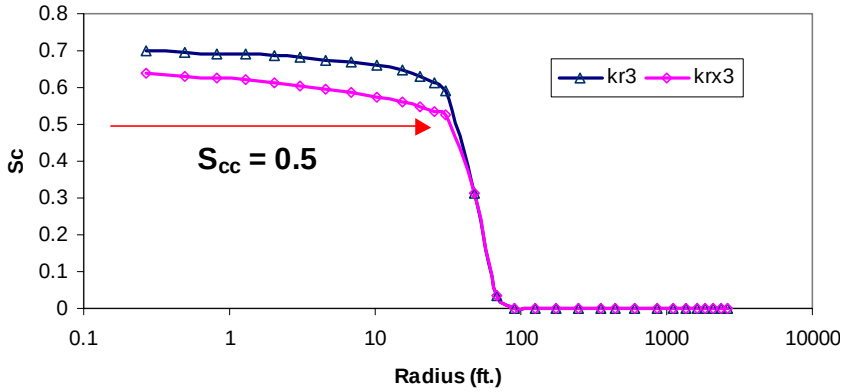

Figure 4.3: Saturation profile across reservoir for Corey (Δ) and X-curves (◊) at S_{cc} = 0.3.

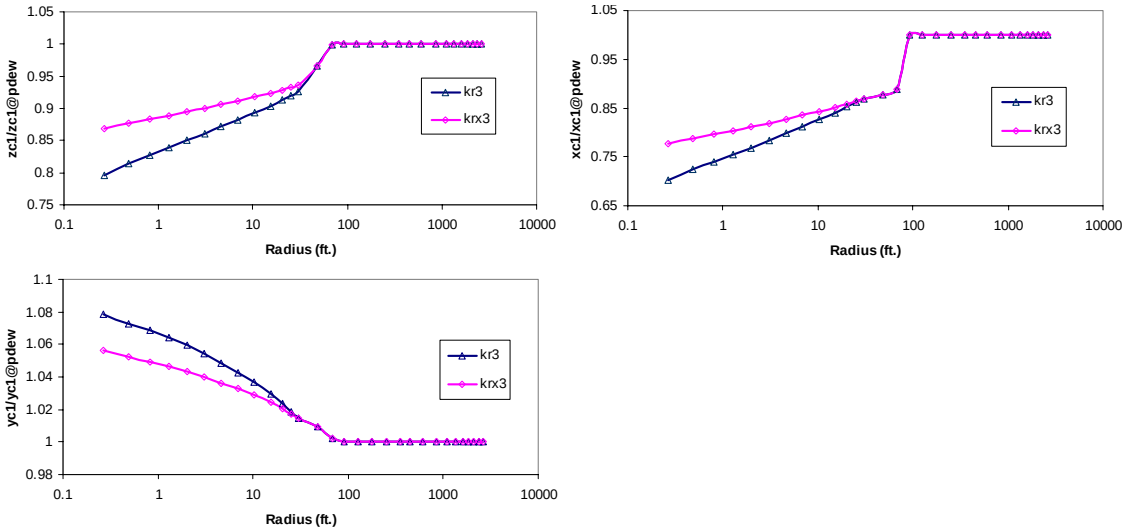

Figure 4.4: C_1 compositional change across reservoir for Corey (Δ) and X-curves (◊) at S_{cc} = 0.5.

4.1.2. Critical Condensate Saturation

The critical condensate saturation was varied between 0 to 50% and the resulting effect on saturation profile and compositional change is shown. For this case, all the parameters including the relative permeability curve were kept the same and the S_{cc} was varied. Figure 4.5 shows the saturation profile across the reservoir for Brooks-Corey relative permeability curves. The resulting compositional change is shown in Figure 4.6. It can be seen that the overall composition change is more for higher S_{cc}, which in turn means larger Region 2.

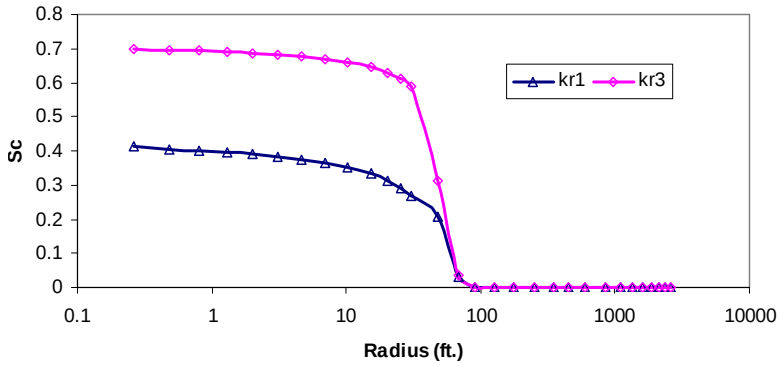

Figure 4.5: Saturation profile across reservoir for Corey curves and Scc = 0 (Δ) and 0.5 (◊).

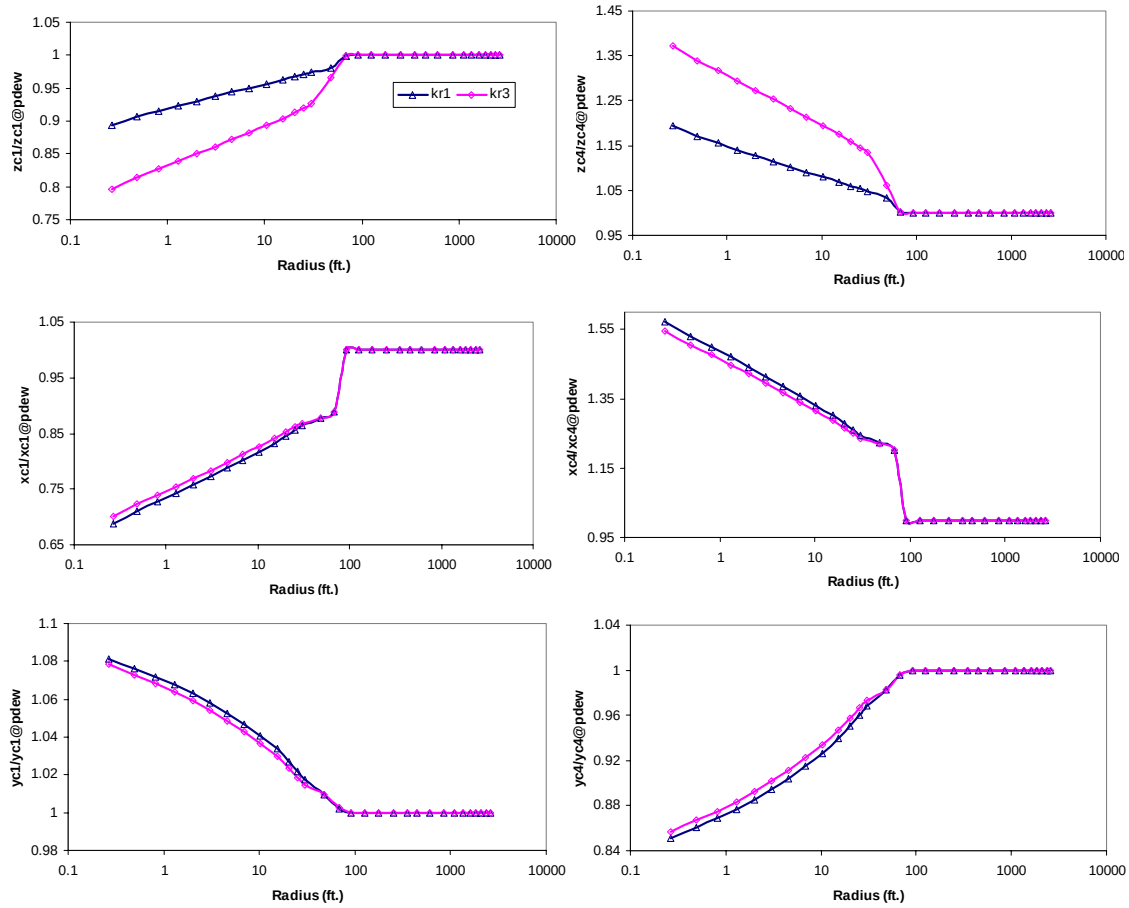

Figure 4.6: C_1 and C_4 compositional change across reservoir for Corey curves at S_{cc} = 0 (Δ) and 0.5 ($\Diamond$).

It is the overall composition that defines the phase behavior of the fluid. Hence, it is found that critical condensate saturation is significant in the extent to which the compositions of the reservoir fluid will change. This is important, as we know that the phase envelope of the reservoir fluid changes with production time. Thus, we would expect the locus of critical points of the fluid to move more in case of higher S_{cc}.

Figure 4.7 and 4.8 show the saturation profile and the resulting changes in composition respectively for the X-curves. We see that the saturation buildup is less in the case when the fluids do not interact with each other. However, the critical condensate saturation has the same effect as seen in case of Corey-curves, even as the changes in composition are less in this case. It is also observed that even though the overall compositions change,

changes in S_{cc} do not affect the liquid and vapor mole fractions. This may be due to the fact that the liquid and vapor phase do not interact during the flow.

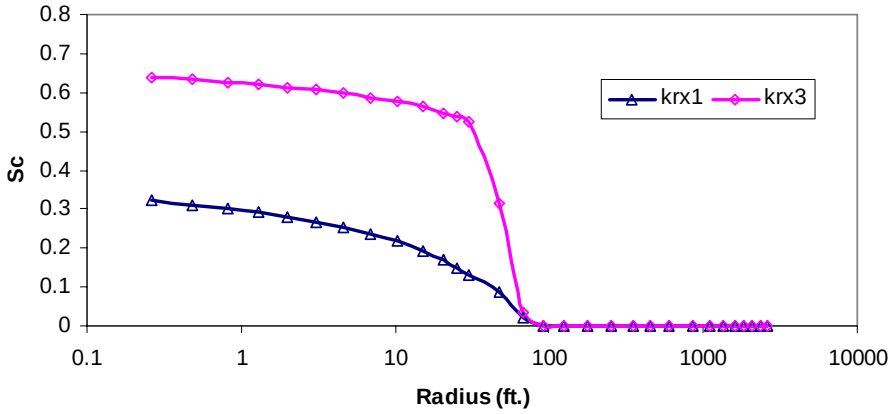

Figure 4.7: Saturation profile across reservoir for X curves and Scc = 0 (Δ) and 0.5 (◊).

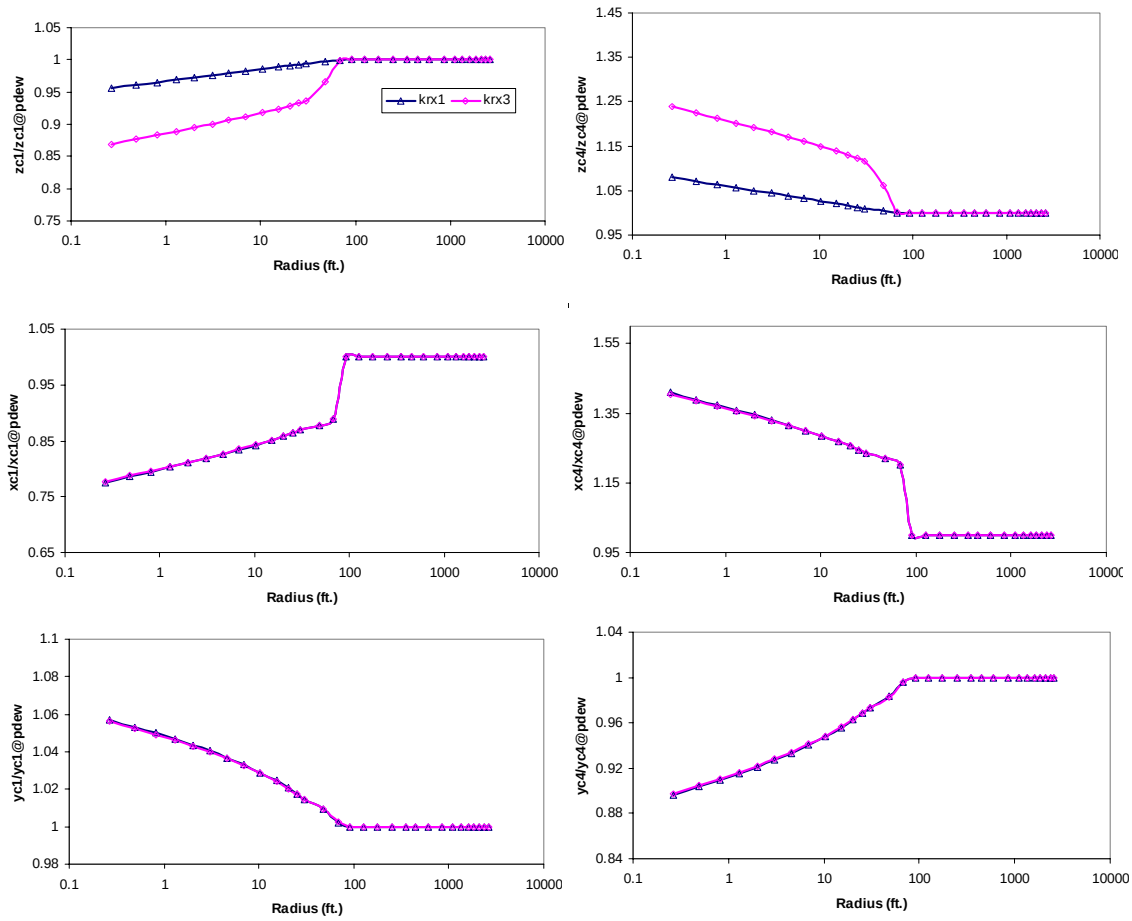

Figure 4.8: C_1 and C_4 compositional change across reservoir for X curves at S_{cc} = 0 (Δ) and 0.5 (◊).

4.2. Varying Production Rates

The effect of varying rate of production was also investigated. Increasing the production rate will result in greater drop in the pressure across the reservoir. We analyzed the final pressure in the wellblock cell and the resulting liquid saturation were compared with the quality lines on the phase envelope at the same pressure. Table 4.1 shows the different flow rate r1 through r7 in lb-mole/day.

Table 4.1: Different flow rates in lb-mole/day used for simulation.

Rate	q_t lb-mole/day
r1	2000
r2	4000
r3	6000
r4	8000
r5	10000
r6	12000
r7	14000

Figure 4.9 shows the pressure and saturation profile across the reservoir for different rates. It is observed that the saturation buildup is different for same pressure drop at different rates. As the rate is increased, the saturation buildup is less for a given pressure drop. For example the Sc at 2500 psi is 57%, 54.5%, and 52% for rates of r3, r5, and r7 respectively. The lesser saturation buildup at increased rate might be due to the "velocity stripping" (Mott et al., 1999) effect as has been documented in literature. This is also seen in Figure 4.10, which is a plot of pressure versus saturation. The saturation increases to a maximum value and then decreases as the pressure is reduced further. Table 4.2 shows the final saturation value in the first grid block along with the grid pressure. It is observed that even though the pressure in case of r7 has dropped to 1282 psi, the saturation is only marginally less than that for r2, in which case the final pressure is 2745 psi.

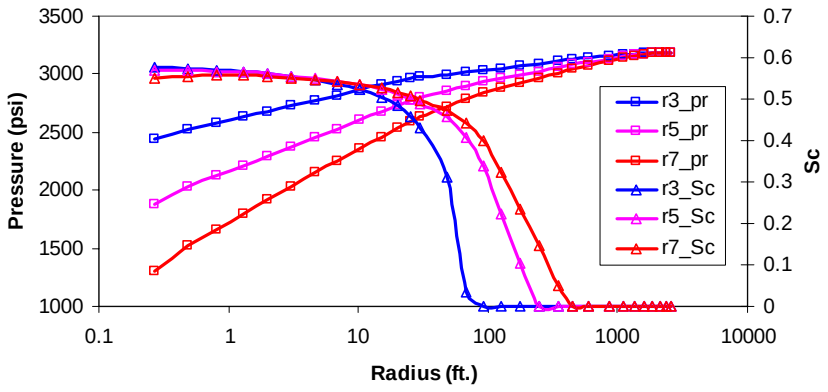

Figure 4.9: Pressure and saturation profile across reservoir for different rates.

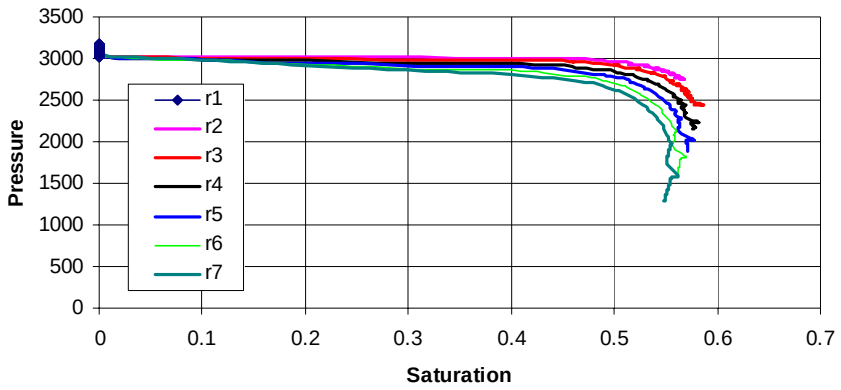

Table 4.10: Pressure versus saturation profile for different rates of production.

Table 4.2: Final saturation and pressure value in the first grid block.

Rate	r1	r2	r3	r4	r5	r6	r7
Saturation	0.0000	0.5650	0.5787	0.5766	0.5708	0.5621	0.5489
Pressure	3029	2746	2440	2160	1885	1601	1296

Even though varying production rates produce different saturation profile, the final saturation buildup is not affected significantly. However, there is significant change in the fluid composition. Figure 4.11 shows the pressure drop and resulting compositional changes for the C_1 component. Hence, higher rates will have greater impact on compositional change and consequently greater shift in phase envelope.

Figure 4.12 shows the shift in phase envelope of the gas-condensate mixture in the well-block grid for different rates of production. The left most envelope is the original reservoir fluid and the ones to the right of it are for r3, r5, and r7 respectively, after 102 days of production. The points on each curve is the critical point for that phase envelope.

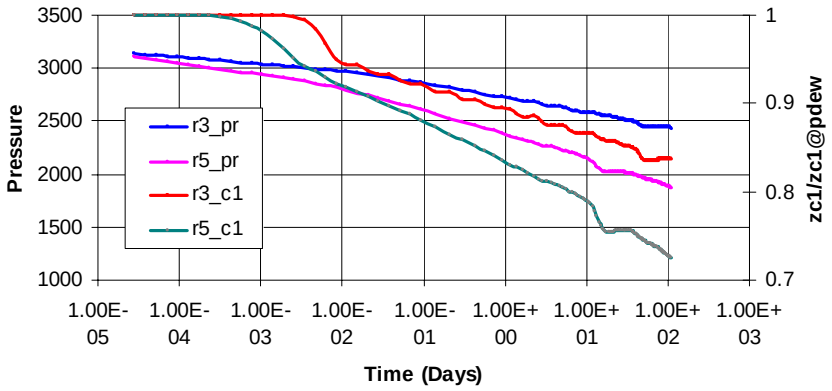

Figure 4.11: Pressure drop and compositional changes across reservoir for different rates of production.

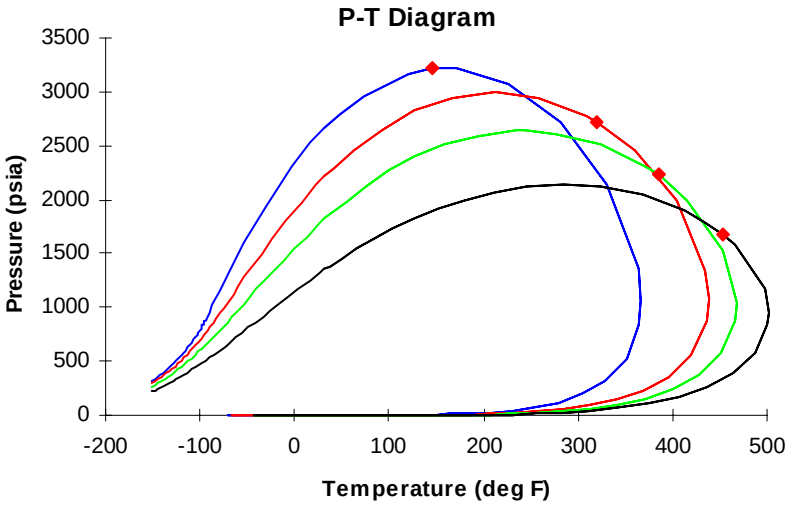

Figure 4.12: Phase envelope of reservoir fluid in well-grid block after 102 days for different constant rates r3, r5, and r7 (original fluid envelope is the leftmost plot).

4.3. Laboratory Scale Simulation

A Cylindrical core plug will be used to carry out actual physical experiments in the laboratory. However, the flow being linear, for simulation purpose, the core will be approximated as a cubical bar whose cross-sectional area is equal to the circular cross sectional area of the core plug. Hence, it will have the same pore volume and hence the same amount of reservoir fluid as the cylindrical plug. The Same fluid mixtures were used in this case and the production was carried at constant total molar rate. The production was adjusted so as to produce the desired pressure drop (comparable to the field case) throughout the core. The total time of simulation was about 0.183 hours (11 minutes).

It was observed in the core plug simulation that the pressure drop occurs almost simultaneously in all the grid blocks. This might be due to the small size of the core and the time steps being very small. Figure 4.13 shows the saturation buildup with time in the first grid block. The result is for fluid 2 and the final saturation buildup is significantly less than that in the field case for the same pressure drop.

The final saturation buildup for the same fluid mixture and the same pressure drop in the field scale simulation was about 41%, while in this case it was about 20%.

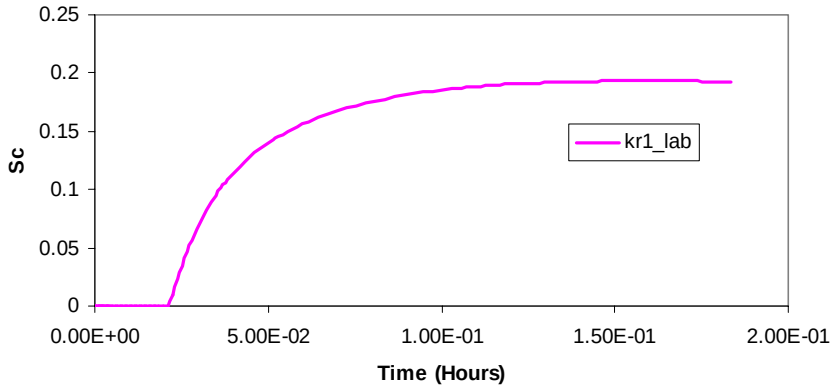

Figure 4.13: Saturation profile over time plot for the first grid block (fluid 2).

As the two simulations are on different time scales, we plotted a pressure versus saturation profile to see the effect of linear flow on the final saturation buildup. Figure 4.14 shows one such plot. It is observed that for almost the same pressure drop, the saturation buildup in the core plug (linear flow) is much less than that in the field scale (radial flow).

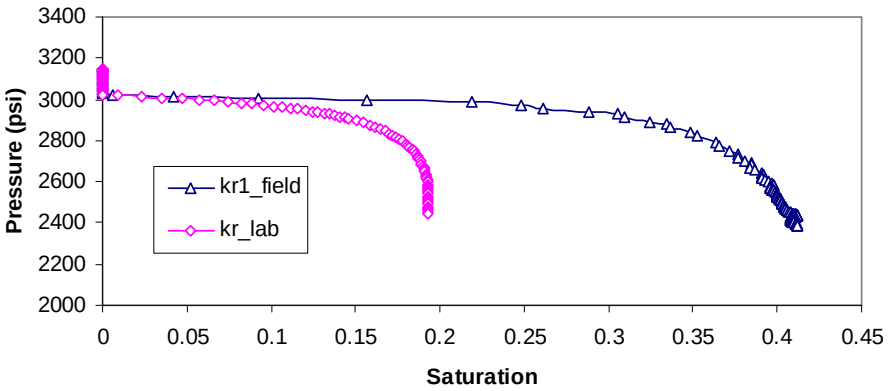

Figure 4.14: Pressure saturation profile for laboratory and filed scale simulation (fluid 2).

This is quite significant and it was observed for other fluid mixtures too. For example for fluid 5, the field and laboratory scale maximum saturations are 57% and 39% respectively. Also, the resulting changes in composition of the fluid mixture in the laboratory case was different from field simulation results. Figure 4.15 shows the compositional change of C_1 fraction of the mixture in field and laboratory scale as a function of pressure drop.

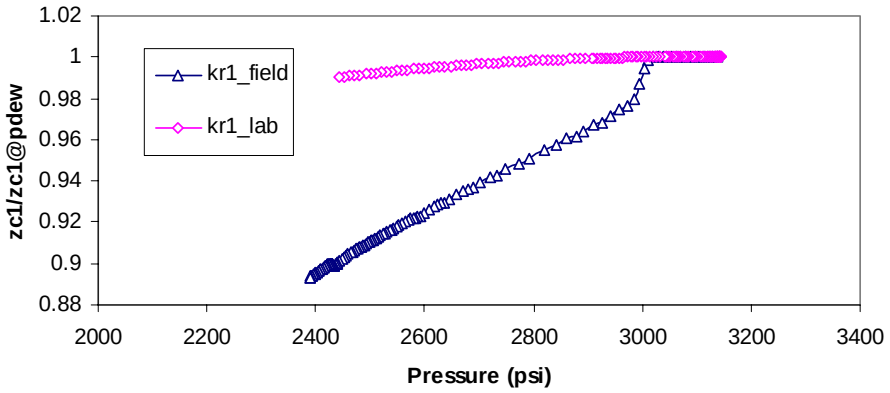

Figure 4.15: C_1 overall composition change with pressure drop for laboratory and field scale (fluid 2).

There is significant difference in the change of the composition of the fluid in the two cases. However, the change in liquid and vapor composition of C_1 is the same in the two cases. Hence, the reason for significant change in overall composition is due to the difference in liquid dropout in the two cases. Thus, the shift in phase envelope of the original reservoir fluid in the laboratory scale simulations is not much and for all practical purpose in the laboratory scale simulations the original reservoir phase envelope will be a fair approximation throughout the simulation.

We can conclude that it is not just the drop in pressure that affects the change in fluid composition. There are other factors such as saturation buildup (liquid dropout) and we see that a dropout of about 20% does not change the phase envelope of the fluid. Thus, if we expect a saturation buildup of this order at field scale, this might not result in any significant shift of phase envelope.

4.4. Constant Bottom Hole flowing Pressure (BHFP)

To investigate the flow phenomenon as pressure drops isothermally in the phase envelope, the production was carried with bottom hole pressure control mode. In this case, the wellblock saturation develops instantaneously as the bottom hole flowing pressure falls below the dew-point. Different bottom hole flowing pressure values were used, which lie along the isothermal pressure decline path in the phase envelope. Figure 4.16 shows the saturation profile for fluid 2 across the reservoir for Brooks-Corey and the X-curves for S_{cc} = 0.3 and bottom hole flowing pressure of 2500 psi.

The nature of the saturation profile is different as observed for constant rate simulation. However, the two curves cross each other at the S_{cc} value (0.5 in this case) and the Corey curves result in higher saturation buildup than X-curves, similar to the constant rate case. This is also true for fluid 5, in which case, even though the nature of saturation profile is different, the two curves cross each other at the S_{cc} value.

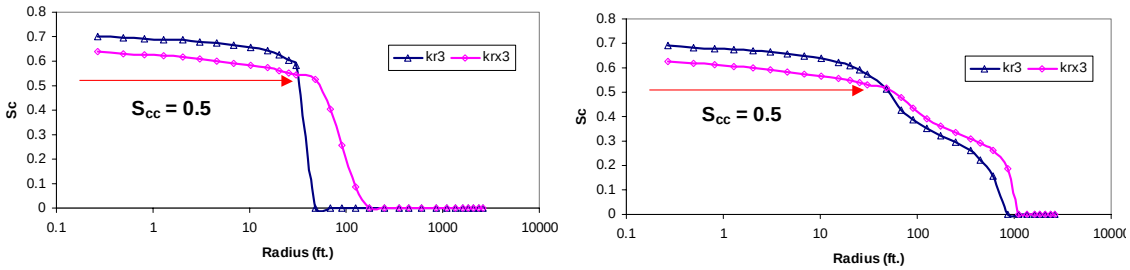

Figure 4.16: Saturation profiles for fluids 2 (left) and 5 (right) for Corey (Δ) and X-curves (◊) at S_{cc} = 0.5 and constant bottom hole flowing pressure.

Figure 4.17 shows the cumulative gas production for the two sets of relative permeability curves (Corey and X-curves) for constant bottom hole flowing pressure. Even though the two result in almost same pressure drop across the reservoir, the cumulative gas production in case of the X-curve is significantly higher than for the Corey-curves.

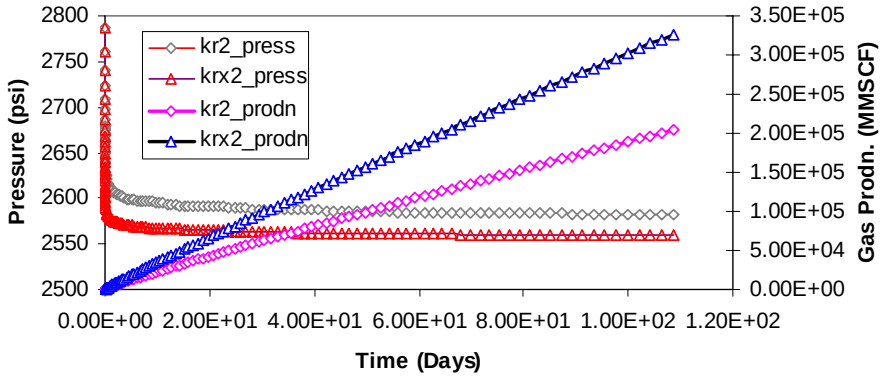

Figure 4.17: Cumulative gas production and pressure curve for Corey and X-curves for bottom hole flowing pressure = 2500 psi (fluid 2).

4.4.1. Capillary Pressure

Capillary pressure was introduced in the relative permeability table of the Eclipse input data file to investigate its effects on the saturation profile and flow. The equations and the plots of different capillary pressures used for simulation purpose have already been shown in Section 3.3.2.

Figure 4.18 shows the saturation profile and the resulting compositional change in C_1 fraction across the reservoir for different capillary pressures. It is observed that, the higher the capillary pressure, the greater is the saturation buildup. Increasing the capillary pressure did not show much effect on the change in mole fraction.

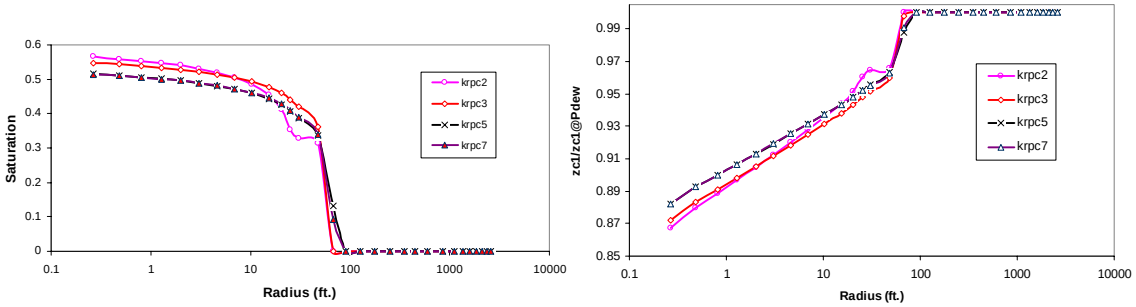

Figure 4.18: Saturation profile and C_1 overall mole fraction for different capillary pressures (fluid 2).

Figure 4.19 shows the cumulative gas production for different capillary pressures. The different capillary pressures have been obtained for different values of pore size distribution index, λ. Pore size distribution index λ is associated with the heterogeneity of rock at the core scale. The greater the pore size distribution index, the more homogeneous the rock. Li and Horne (2003) have shown for oil-water systems that the oil recovery by gravity drainage may increase with the pore size distribution index. In this case also, we observe more gas production for higher values of λ (i.e. smaller capillary pressure values).

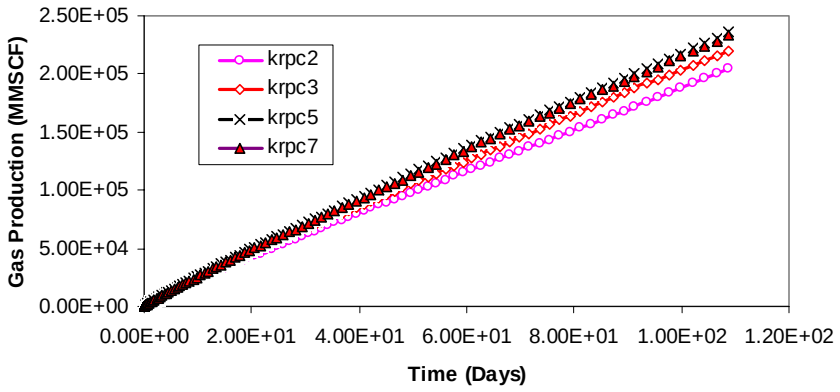

Figure 4.19: Cumulative gas production for different capillary pressure values (fluid 2).

Chapter 5

5. Conclusion

5.1. Conclusions

1. Saturation buildup across a gas-condensate reservoir is much higher than the maximum equilibrium saturation given by the phase behavior of the fluid.

2. The saturation profile for a given critical condensate saturation (S_{cc}) value follows the same path for different relative permeability curves at saturations less than S_{cc}. However, the profile deviates above the S_{cc} value.

3. Compositional changes are more for higher values of critical condensate saturation, S_{cc} (larger Region 2).

4. Saturation buildup depends significantly on the type of relative permeability curves used. Comparisons between Corey-curves and X-curves (no interaction between gas and liquid phases) show that the saturation buildup is less in the case of X-curves. The change in mole fraction is also less when X-curves was used. It was also observed that using different S_{cc} values for the X-curves resulted in different overall composition changes. However, the liquid and vapor mole fraction changes was found to be the same.

5. Comparisons between field (radial flow) and laboratory (linear flow) scale simulations show that the saturation buildup in core plug is significantly less than that in the field case for the same condensate fluid and identical pressure drop.

6. Introduction of capillary pressure in the study showed that higher capillary pressure results in higher saturation buildup and thereby a smaller amount of gas produced. The changes in the composition of the fluid were more for higher

capillary pressure. However, significant difference was observed only for high capillary pressure values. The changes were insignificant when compared between two smaller capillary pressure values.

5.2. Future Work

Critical condensate saturation (S_{cc}) is an imporatnt parameter when we are studying the flow behavior in gas-condensate reservoirs. Laboratory expeiments to determine accurate S_{cc} values at the core scale are required. It has also been observed that there is significant difference between field and laboratory scale saturation buildup. In future work, this should be investigated as to what extent we can predict the saturation profile in a real gas-condensate reservoirs from laboratory results. Relative permeability curves are very significant in any study of fluid flow in gas-condensate reservoirs. Experimental measurement of relative permeability curves needs to be carried out.

Nomenclature

k_{ro} = oil relative permeability

k_{rg} = gas relative permeability

k_{rw} = wetting phase relative permeability

k_{rnw} = non-wetting phase relative permeability

S_w = wetting phase saturation

S_o = oil saturation

S_g = gas saturation

S_w^* = normalized saturation of wetting phase

λ = pore size distribution index

P_c = capillary pressure

p_e = entry capillary pressure

S_{cc} = critical condensate saturation

p_{dew} = dew-point pressure

Abbreviations

GOR = gas-oil raio, *MCF/stb*

OGR = oil-gas ratio, *stb/MCF*

BHFP = bottom hole flowing pressure, *psi*

CCE = constant composition expansion

CVD = constant volume depletion

References

Afidick, D., Kaczorowski, N.J., Srivinas, B.: 1994, Production performance of a retrograde gas reservoir: a case study of the arun field, *SPE paper 28749.*

Ahmed, T.: 1989, *Hydrocarbon phase behavior*, Gulf Publishing Company.

Allen, F.H., and Roe, R.P.: 1950, Performance characteristics of volumetric condensate reservoir, *AIME transaction 189, 83-90*.

Ali, J.K., McGauley, P.J. and Wilson, C.J.: 1997, Experimental studies and modelling of gas condensate flow near the wellbore, *SPE paper 39053.*

Asar, H. and Handy, L.L.: 1988, Influence of interfacial tension on gas-oil relative permeability in a gas-condensate system, *SPE paper 11740.*

Barnum, R.S., Brinkman, F.P., Richardson, T.W. and Spillette, A.G.: 1995, Gas condensate reservoir behavior: productivity and recovery reduction due to condensation, *SPE paper 30767.*

Bertram, D.A., Van de Leemput, L.E.C., McDevitt, B.S. and Al Harthy, N.M.A.: 1997, Experiences in gas-condensate well test analysis using compositional simulation, *SPE paper 37994.*

Coats, K. H.: 1988, Simulation of gas condensate reservoir performance, *JPT* pp. 1870–1886.

Chopra, A. and Carter, R.D.: 1986, Proof of the two-phase steady state theory for flow through porous media, *SPE paper 14472*.

Danesh, A.: 1998, *PVT and phase behavior of petroleum reservoir fluids*, Elsevier.

Danesh, A., Henderson, G.D., Krinis, D., and Peden, J.M.: 1988, Experimental investigation of retrograde condensation in porous media at reservoir conditions, *SPE paper18316.*

Economides, M.J., Schlumberger, D., Dehghani, K, Ogbe, D.O. and Ostermann, R.D.: 1987, Hysteresis effects for gas condensate wells undergoing buildup tests below the dew point pressure, *SPE paper 16748.*

Fevang, Φ. and Whitson, C.H.: 1995, Modelling gas condensate deliverability, *SPE paper 30714.*

Fussel, D. D.: 1973, Single well performance for gas condensate reservoirs, *J. Pet.Tech.* **255**, 860–870.

Gravier, J.F., Lemouzy P., Barroux, C. and Abed, A.F.: 1983, Determination of gas-condensate relative permeability on whole cores under reservoir conditions, *SPE paper 11493.*

Hinchman, S.B. and Barree, R.D.: 1985, Productivity loss in gas condensate reservoirs, *SPE paper 14203.*

Jones, J.R., Vo, D.T. and Raghavan, R.: 1989, Interoperation of pressure buildup responses in gas condensate wells, *SPE paper 15535.*

Li, K. and Horne, R.N.: 2003, Numerical simulation with input consistency between capillary pressure and relative permeability, *SPE paper 79716.*

Nikravesh, M., Soroush, M.: 1996, Theoretical methodology for prediction of gas-condensate flow behavior, *SPE paper 36704.*

O'Dell, H.G. and Miller, R.N.: 1965, Successfully cycling a low-permeability, high-yield gas condensate reservoir, *SPE paper 1495*.

Raghavan, R., Chu, W. C. and Jones, J. R.: 1995, Practical considerations in the analysis of gas-condensate well tests, *SPE paper 30576*.

Roebuck, I. F., Jr., Ford, W. T., Henderson, G. E. and Douglas, J., Jr.: 1969, The compositional reservoir simulator: case III – the radial geometry, unpublished paper, available from Core Laboratories, Inc., Dallas, Texas

Rousennac, B.: 2001, *Gas condensate well test analysis*, MS thesis, Stanford University.

Saeidi, A. and Handy, L.L.: 1974, Flow and phase behavior of gas condensate and volatile oils in porous media, *SPE paper 4891.*

Sigmund, P. M., Dranchuk, P. M., Morrow, N. R. and Purvis, R. A.: 1973, Retrograde condensation in porous media, *SPE paper 3476.*

Sognesand, S.: 1991, Long-term testing of vertically fractured gas condensate wells, *SPE paper 21704.*

Thompson, L., Niu, J. G. and Reynolds, A.: 1993, Well testing for gas condensate reservoirs, *SPE paper 25371*.

Whitson, C.H. and Brule, M.R.: 2000, Phase behavior, *Monograph/SPE volume 20, Henry L. Doherty series*.

Xu, S. and Lee, J. W.: 1999, Two-phase well test analysis of gas condensate reservoirs, *SPE paper 56483*.

Appendix A

A. Eclipse input data file (Field scale)

```
-- ================================================================================
RUNSPEC
-- ================================================================================
--NOSIM

FIELD

RADIAL

-- NO Water is present

--WATER

--AIM solution method: Adaptative implicit

AIM

--3 components in study ( plus water )

COMPS
3 /

--Peng-Robinson equation of state to be used

EOS

PR/

DIMENS
-- NR NTHETA NZ
  30  1    1 /

-- ... tables
TABDIMS
-- NTSFUN NTPVT NSSFUN NPPVT NTFIP NRPVT -nu-  NTENDP
      1     1     80     1*    1    1*    1*     1*  /

-- ... wells and groups
WELLDIMS
-- MWMAXZ  NCWMAX  NGMAXZ  NWGMAX
     1       1       1       1    /

-- Single phase fluid is a gas:

ISGAS
```

```
MULTSAVE
1 /
FMTOUT
UNIFOUT

-- ======================================================================
GRID
-- ======================================================================
INIT

INRAD
.25 /
DR
0.53000     0.4429     0.6539     0.9655     1.4255     2.1046     3.1072
4.5876     6.7732    10.0000    10.0000     10 10 35.0000  40.0000
 47    68    100    150    200 200 300 500   500 500 500 500 500 500 500
/

--
EQUALS
DTHETA
360 /
DZ
30 /
TOPS
7000/

PORO
0.20 /
/


PERMR
30*5 /
PERMTHT
30*0 /



-- ======================================================================
EDIT
-- ======================================================================

-- ======================================================================
PROPS
-- ======================================================================

-- Include File with Fluid Description
INCLUDE
FLUIDPVT.INC
/

-- degree F
RTEMP
222/
```

```
-- Include KR tables to be used
INCLUDE
kr2.INC
/

--Rock and water pressure data
ROCK
4036 0.000004 /

PVTW
4036 1.0 0.000003 0.31 0.0 /

--Surface density of water

DENSITY
1* 63.0 1* /

-- ======================================================================
SOLUTION
-- ======================================================================
EQUALS
PRESSURE
3190 /
SWAT
0 /
SGAS
1 /
/

ZMF
30*.75
30*.20
30*.05
/


-- OUTPUT of the grid values in .FUNRST at each specified TSTEP
OUTSOL
PRES SOIL XMF YMF VMF VOIL VGAS BOIL BGAS DENO DENG KRG KRO ZMF /

-- No output in .PRT except TSTEP convergence summary
RPTPRINT
13*0/

-- ======================================================================
SUMMARY
-- ======================================================================
RUNSUM
RPTONLY


-- Data needed for computation for Sand face Integral
WBHP
P/
WBP
```

```
P/


INCLUDE
'BSOIL.txt'/

INCLUDE
'BPR.txt'/

FPPG
/
FPPO
/

WGOR
P/
BKRO
1 1 1/
/
BKRG
1 1 1/
/
BVOIL
1 1 1/
/
BVGAS
1 1 1/
/
BBOIL
1 1 1/
/
BBGAS
1 1 1/
/

-- Other usefull Info
BDENO
1 1 1/
/
BDENG
1 1 1/
/
INCLUDE
'BVMF.txt'/
/
WXMF
P 1 /
P 2 /
P 3 /
/
WYMF
P 1 /
P 2 /
P 3 /
/
WZMF
```

```
P 1 /
P 2 /
P 3 /
/
INCLUDE
'BXMF.txt'/

INCLUDE
'BYMF.txt'/

WHMPR
P/
WOPR
P/
WGPR
P/
WWGPR
P/
WGDN
P/
WCHMR
P 1/
P 2/
P 3/
/

-- ================================================================================
SCHEDULE
-- ================================================================================
-------- THE SCHEDULE SECTION DEFINES THE OPERATIONS TO BE SIMULATED
--------------------------------------------------------------------------------

--PSEUPRES
--PICOND
--3*/

SEPCOND
SEP FIELD 1 60 14.7 /
/
--Define the production well

WELLSPEC
P FIELD 1 1 1*  SEP/
/

COMPDAT
--name i j k1 k2 flag sat.tab trans id kh skin D dir
   P   1 1 1  1 'OPEN' 1*      1*    .5 1*  0    1* 'Z'/
/

WELLPROD
P TM 4* 500 5* 6000 /
/


TUNING
```

```
1.1574E-6  1.1574E-1  1.1574E-7  1*  1.1  0.5   /
 /
 /
INCLUDE
'TIMESTEP2.txt'/


END
```

B. Eclipse input data file (Core scale)

```
-- ================================================================
RUNSPEC
-- ================================================================
--NOSIM
LAB

CART
AIM
-- 3 COMPONENT IN STUDY

COMPS
3/

-- Peng-Robinson equation of state to be used

EOS
PR/

DIMENS    -- dimensions of the model
--NDIVIX NDIVIY NDIVIZ
30 1 1/

TABDIMS
1 1 80 1* 1 1* 1* 1*/

WELLDIMS
2 1 1 1/
-- Single phase fluid is a gas:

ISGAS

MULTSAVE
1/

FMTOUT
UNIFOUT
```

```
START     -- starting date for simulation run
  16 'APR' 2002 /



GRID      == geometry of our model ====================================

INIT

DXV
3*0.1 3*0.2 3*0.5 3*0.75 3*1 15*1.5/

DYV
4.483/

DZV
4.483/



PERMX
30*5
/

PERMY
30*0/

PERMZ
30*0/

TOPS
30*1/

PORO
30*0.2/

-- ===========================================================================
EDIT
-- ===========================================================================
-- ===========================================================================
PROPS
-- ===========================================================================
-- Include File with Fluid Description


INCLUDE
FLUIDPVT_LAB.INC
/


-- Reservoir temperature: Deg C
RTEMP
90.55  /


-- Include KR tables to be used
```

```
INCLUDE
kr2.INC
/

-- Rock and fluid properties

ROCK
300.0  0.00000000001  /



--Surface density of water

DENSITY
1* 0.997 1* /

-- ================================================================================
SOLUTION
-- ================================================================================
--EQUALS
PRESSURE
30*217 /
SWAT
30*0 /
SGAS
30*1 /
/

ZMF
30*.75
30*.20
30*.05
/

-- OUTPUT of the grid values in .FUNRST at each specified TSTEP
OUTSOL
PRES SOIL XMF YMF VMF VOIL VGAS BOIL BGAS DENO DENG KRG KRO ZMF /

-- No output in .PRT except TSTEP convergence summary
RPTPRINT
13*0/

-- ================================================================================
SUMMARY
-- ================================================================================
RUNSUM
RPTONLY
-- Data needed for computation for Sand face Integral
WBHP
P/
WBP
P/

INCLUDE
'BSOIL.txt'/
```

```
INCLUDE
'BPR.txt'/
/
FPPG
/
FPPO
/

WGOR
P/
BKRO
1 1 1/
/
BKRG
1 1 1/
/
BVOIL
1 1 1/
/
BVGAS
1 1 1/
/
BBOIL
1 1 1/
/
BBGAS
1 1 1/
/

-- Other useful Info
BDENO
1 1 1/
/
BDENG
1 1 1/
/
INCLUDE
'BVMF.txt'/
/
WXMF
P 1 /
P 2 /
P 3 /
/
WYMF
P 1 /
P 2 /
P 3 /
/
WZMF
P 1 /
P 2 /
P 3 /
/
INCLUDE
'BXMF.txt'/
```

```
INCLUDE
'BYMF.txt'/

WHMPR
P/
WOPR
P/
WGPR
P/
WWGPR
P/
WGDN
P/
WCHMR
P 1/
P 2/
P 3/
/

-- ======================================================================
SCHEDULE
-- ======================================================================
-------- THE SCHEDULE SECTION DEFINES THE OPERATIONS TO BE SIMULATED
----------------------------------------------------------------------

--PSEUPRES
--PICOND
--3*/

SEPCOND
SEP FIELD 1 15.6 1 /
/
--Define the production well

WELLSPEC
P FIELD 1 1 1*  SEP/

/

COMPDAT
--name i j k1 k2 flag sat.tab trans id kh skin D dir
   P   1 1 1  1 'OPEN' 1*     1*   .015 1*  0   1* 'Z'/

/


--Well P set to target total molar rate of 7000lb-mole/d,
--with min bhp of 60 atm

--WCONPROD
--P OPEN GRAT 2* 100000 2* 60 /
--/

WELLPROD
P TM 4* 70 5* 1/
```

```
/


TUNING
1.1574E-6  1.1574E-1  1.1574E-7  1*  1.1  0.5   /
 /
 /
INCLUDE
'timestep_lab.txt'/

END
```